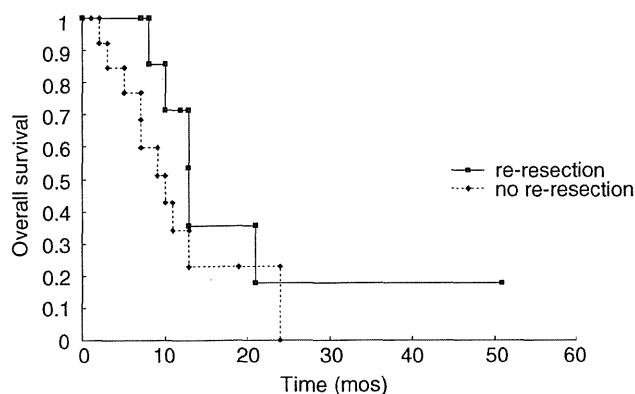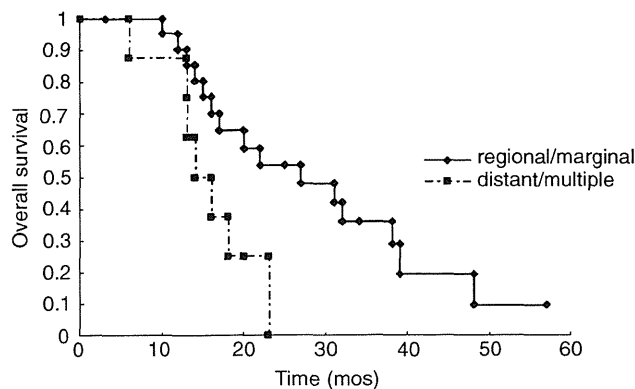Fig. 3 Follow-up images in 4 patients with glioblastoma initially located in the prefrontal region showing the recurrent tumor affected the genu of the corpus callosum (*arrows*).

Fig. 4 Comparison of the overall survival from the time of regional or marginal tumor progression relative to re-resection. There is no significant difference (p = 0.20).

Fig. 5 Comparison of the overall survival from the time of surgery in patients with different recurrence patterns of intracranial glioblastoma. There is a significant difference (p = 0.04).

was better after complete tumor removal compared to partial removal or biopsy.[51] Resection of 98% or more of glioblastoma is associated with significant improvement of the long-term outcome,[19] whereas the same trend was recently revealed even at 78% resection rate.[39] Concordant results were reported by The Committee of Brain Tumor Registry of Japan: analysis of 5,328 cases of glioblastoma showed that more than 95% tumor removal is associated with survival advantage, but such resection rate was attained in only 31.4% of cases.[5] In our series, 95% and more resection was achieved in 47 of 65 consecutive patients (72%). After aggressive surgery and adjuvant management 23% of patients remained free of tumor progression within the median follow-up period of 17 months. Such beneficial results may reflect the advantages of our treatment concept of information-guided surgery for brain tumors based on the constant use of advanced intraoperative technologies.[17,28,30]

Our surgical strategy for information-guided management of intracranial gliomas with the use of iMR imaging has been described in detail elsewhere.[27,28,30] It is based on the integration of various intraoperative anatomical, functional, and histological data to attain maximal surgical resection of the tumor with minimal risk of postoperative neurological morbidity. It should be specifically emphasized that complete removal is highly desirable, but is not the ultimate goal of surgery for glioma. In our practice, the procedure is usually directed to the maximal possible resection of the enhanced area in cases of high-grade glioma, which might be radiologically total as well as subtotal, leaving the residual lesion within the functioning eloquent brain structures identified with neurophysiological monitoring and/or brain mapping.[27,28,30]

In the majority of reported series, local progression of intracranial glioblastoma after initial

Table 3 Recurrence rates of intracranial glioblastoma after treatment

Author (Year)	No. of analyzed cases	Cohort characterization	Length of follow-up (mos)	Total recurrence rate	Local recurrence rate
Hochberg and Pruitt (1980)[12]	42	CT-based delineation of the tumor recurrence after irradiation and/or chemotherapy (CCNU); Anaplastic astrocytomas might be included	ND	ND	80%
Nagashima et al. (1989)[32]	48	Comparison of 3 FRT techniques with irradiation dose >45 Gy in each case: WBRT, generous local irradiation (complete coverage of the area of hypodensity on CT), and restricted local irradiation (within 2 cm of the CT-defined tumor margin)	ND	100%	85%
Sneed et al. (1994)[43]	25	Surgery, FRT (59.4–60 Gy) with concomitant oral hydroxyurea followed by brachytherapy with high-activity (50 Gy) iodine-125 sources and 6 cycles of chemotherapy (procarbazine, lomustine, and vincristine)	ND	88%	68%
Nakagawa et al. (1998)[33]	38	Surgical resection or biopsy in all cases (gross total resection 8%), followed by FRT (60–90 Gy in 20 cases and ≥90 Gy in 16) concurrent with chemotherapy (ACNU and vincristine)	ND	84%	53%
Oppitz et al. (1999)[35]	34	CT-based analysis of recurrence after FRT (range of total doses 45–68 Gy, median 60 Gy)	ND	100%*	97%
Wick et al. (2008)[54]	63	Comparison of recurrence patterns in only radiotherapy group (33 cases) and TMZ-based chemoradiotherapy group (30 cases); "Debulking surgery" was done in 37 patients	ND	100%*	80%
Brandes et al. (2009)[2]	95	Total or subtotal surgical resection followed by TMZ-based chemoradiotherapy (irradiation dose 60 Gy)	median 18.9; range 6.6–44.8	83%	72%
Milano et al. (2010)[25]	54	Surgical resection or biopsy (gross total resection 31%), followed by TMZ-based chemoradiotherapy (irradiation dose 60 Gy); Additional SRS boost in 3 patients	median 17	72%	67%
Chamberlain (2011)[3]	70	Initial treatment with FRT with concurrent and adjuvant TMZ followed by bevacizumab at first recurrence	ND	100%*	80%
McDonald et al. (2011)[23]	62	Evaluation of the limited margin FRT (total dose 60 Gy); Gross total tumor resection in 45% of patients; Concurrent and adjuvant chemotherapy with TMZ (97% of patients) or concurrent arsenic trioxide (3% of patients)	median 12; maximal 28	69%	68%
Oh et al. (2011)[34]	67	Evaluation of recurrence patterns after TMZ-based chemoradiotherapy; Tumor "resection" in 13% of patients	ND	100%*	87%
Murakami et al. (2012)[31]	138	Maximal possible tumor removal (gross total resection in 28% of patients) followed by FRT (dose 60 Gy) with concurrent and adjuvant chemotherapy	ND	96%	88%
Pan et al. (in press)[36]	31	Overall 10 patients underwent total surgical resection; In 10 cases maximal tumor removal followed by FRT (59.4–60.0 Gy) with concurrent and adjuvant TMZ was done; 12 patients were treated with intracavitary brachytherapy after maximal surgical debulking followed by FRT (45 Gy) with concurrent and adjuvant TMZ; 9 patients had unresectable disease and underwent hypofractionated radiotherapy (50–66 Gy in 10 fractions) followed by adjuvant TMZ or bevacizumab	median 12.6; range 3.5–50.6	100%	52%
Present series	43	≥95% surgical resection in all cases (total resection 51%) followed by FRT (60 Gy) with chemotherapy (ACNU or TMZ) or vaccine therapy	median 17; range 3–71	77%	51%

*Series included only cases with recurrences.   ACNU: nimustine, CT: computed tomography, CCNU: lomustine, FRT: fractionated radiotherapy, ND: no data, SRS: stereotactic radiosurgery, TMZ: temozolomide, WBRT: whole brain radiation therapy.

management was encountered in 67% to 97% of cases (Table 3),[2,3,12,23,25,31,32,34,35,43,54] but comparison of different studies is difficult due to differences in treatment strategy, proportion of patients with total surgical tumor removal, postoperative surveillance, length of follow-up, as well as definition and categorization of the tumor progression. Nevertheless, aggressive resection of the neoplasm may

change its recurrence pattern.[11,31] In a recent study, regional re-growth of glioblastoma after surgery and chemoradiotherapy was noted in 100% of biopsied and 97% of partially removed lesions, but in just 62% of lesions after gross total resection.[31] Moreover, in 10% of the latter cases, PFS for more than 24 months was marked, which is more or less comparable to the present results. We were able to identify two other series which demonstrated similar outcomes. High-dose FRT (from 60 to more than 90 Gy) concurrent with chemotherapy (ACNU, vincristine) resulted in 53% local recurrence rate.[33] In another series aggressive management, including total tumor removal (32% of cases), brachytherapy, and hypofractionated radiotherapy, resulted in 52% local tumor progression within a median follow up of 12.6 months.[36] Based on these findings, we suggest that aggressive management with gross total resection and/or high dose irradiation may result in improvement of local control of intracranial glioblastoma.

In cases of malignant glioma infiltration of the tumor cells can be identified far beyond the localized contrast-enhanced area identifiable on MR imaging. Therefore, comprehensive evaluation of the distant spread of neoplasm is necessary in each individual case,[36] and can be possibly attained with detailed analysis of fluid-attenuated inversion recovery or T_2-weighted MR images, as well as functional and metabolic information obtained with perfusion-weighted, diffusion-weighted, and diffusion tensor imaging, or with ^{1}H-MR spectroscopy.[13,54] Such distant tumor spread may vary from one patient to another, and aggressive local management, including surgery and irradiation, can be expected to have greater efficacy for more localized disease. Correspondingly, regional or marginal tumor progression after initial total or nearly total resection of glioblastoma followed by postoperative FRT should appear later compared to distant recurrences, which are affected only by systemic therapy. However, this was not confirmed in the present study, since PFS did not differ significantly between the two groups of patients. Previously, similar PFS was found in patients with local and distant recurrences of glioblastoma,[34] whereas some series demonstrated that time to regional tumor progression might be even shorter compared to distant failure.[25,31,36]

At present, the standard management of glioblastoma includes chemotherapy with temozolomide concomitant and adjuvant to FRT.[46,47] This treatment is not complication-free,[15] which is enforcing the search for novel therapeutic options for malignant gliomas. Interest is growing in modalities based on tumor-specific immune reactions, which

have potentially high benefit-to-risk ratio. Our recent prospective study on the use of AFTV concomitant with FRT for management of newly diagnosed glioblastoma showed very promising results.[29] In the present analysis, the recurrence patterns did not differ between patients, who underwent chemotherapy or vaccine therapy, so both types of adjuvant management may have comparable efficacy in control of the tumor progression after initial treatment. However, systemic therapy in general may have rather limited effect on the recurrence pattern of glioblastoma, as distant failure was noted in 18% of patients in the temozolomide-based chemoradiotherapy group, and 23% of those ones in FRT only group.[54]

The present study did not identify any clinical factor associated with specific recurrence patterns of intracranial glioblastoma. However, all tumors initially located in the prefrontal region at the time of further progression invariably affect the genu of the corpus callosum. Therefore, routine inclusion of this area into the irradiation field after total or near total surgical resection of such neoplasms might be reasonable. Several previous studies found that local recurrence of glioblastoma was associated with impaired prognosis.[2,12,25,44] In particular, the median survival was 17.3, 14.8, and 26.1 months in patients with recurrence inside, at the margin, and outside the irradiation field.[2] In contrast, our 22 patients with regional or marginal progression of the tumor had significantly longer (p = 0.04) OS compared to patients with distant or multiple recurrences. Corresponding OS rates were 90% vs. 75% at 1 year and 54% vs. 0% at 2 years after surgery. Such trends might reflect selection bias with more aggressive salvage treatment, particularly re-resection, or inclusion of some cases with pseudoprogression erroneously interpreted as local recurrence, which might result in survival advantage.

Modifications of clinical practice during the study period represent unavoidable pitfall of any retrospective investigation, but seemingly did not affect the results of the present study. On the other hand, absence of volumetric tumor assessment might lead to somewhat inaccurate estimation of the resection rate. Nevertheless, the criteria for total removal were rather strict, since any contrast-enhanced area on postoperative MR imaging obtained within 3 days after surgery was considered to be residual neoplasm.[8] In fact, visual side-by-side comparison of MR images still represents a rather common method for the evaluation of treated intracranial tumors, but is less accurate compared to more sophisticated tools.[9] According to recent recommendations of the Response Assessment in Neuro-Oncology Working

Group, volumetric methods for postoperative evaluation of gliomas are not ultimately required at present and still considered as a field of major research.[22,52]

In conclusion, aggressive surgical resection and adjuvant management of intracranial glioblastoma may change its recurrence patterns. Further tumor progression appears in the wall of the resection cavity or within 2 cm from its margin in approximately half of such patients. This group has a trend for longer OS compared to patients with distant or multiple recurrences.

Acknowledgements

References

1) Albert FK, Forsting M, Sartor K, Adams HP, Kunze S: Early postoperative magnetic resonance imaging after resection of malignant glioma: Objective evaluation of residual tumor and its influence on regrowth and prognosis. *Neurosurgery* 34: 45–61, 1994

2) Brandes AA, Tosoni A, Franceschi E, Sotti G, Frezza G, Amista P, Morandi L, Spagnolli F, Ermani M: Recurrence pattern after temozolomide concomitant with and adjuvant to radiotherapy in newly diagnosed patients with glioblastoma: Correlation with MGMT promoter methylation status. *J Clin Oncol* 27: 1275–1279, 2009

3) Chamberlain MC: Radiographic patterns of relapse in glioblastoma. *J Neurooncol* 101: 319–323, 2011

4) Chan JL, Lee SW, Fraass BA, Normolle DP, Greenberg HS, Junck LR, Gebarski SS, Sandler HM: Survival and failure patterns of high-grade gliomas after three-dimensional conformal radiotherapy. *J Clin Oncol* 20: 1635–1642, 2002

5) The Committee of Brain Tumor Registry of Japan: Report of brain tumor registry of Japan (1984–2000), 12th edition. *Neurol Med Chir (Tokyo)* 49 Suppl: 1–101, 2009

6) Curran WJ Jr, Scott CB, Horton J, Nelson JS, Weinstein AS, Fischbach AJ, Chang CH, Rotman M, Asbell SO, Krisch RE, Nelson DF: Recursive partitioning analysis of prognostic factors in three Radiation Therapy Oncology Group malignant glioma trials. *J Natl Cancer Inst* 85: 704–710, 1993

7) Dillman RO, Duma CM, Ellis RA, Cornforth AN, Schiltz PM, Sharp SL, DePriest MC: Intralesional lymphokine-activated killer cells as adjuvant therapy for primary glioblastoma. *J Immunother* 32: 914–919, 2009

8) Ekinci G, Akpinar IN, Baltacioglu F, Erzen C, Kilic T, Elmaci I, Pamir N: Early-postoperative magnetic resonance imaging in glial tumors: prediction of tumor regrowth and recurrence. *Eur J Radiol* 45: 99–107, 2003

9) Erickson BJ, Wood CP, Kaufmann TJ, Patriarche JW, Mandrekar J: Optimal presentation modes for detecting brain tumor progression. *AJNR Am J Neuroradiol* 32: 1652–1657, 2011

10) Fabrini MG, Perrone F, De Franco L, Pasqualetti F, Grespi S, Vannozzi R, Cionini L: Perioperative high-dose-rate brachytherapy in the treatment of recurrent malignant gliomas. *Strahlenther Onkol* 185: 524–529, 2009

11) Forsting M, Albert FK, Kunze S, Adams HP, Zenner D, Sartor K: Extirpation of glioblastomas: MR and CT follow-up of residual tumor and regrowth patterns. *AJNR Am J Neuroradiol* 14: 77–87, 1993

12) Hochberg FH, Pruitt A: Assumptions in the radiotherapy of glioblastoma. *Neurology* 30: 907–911, 1980

13) Hou LC, Veeravagu A, Hsu AR, Tse VCK: Recurrent glioblastoma multiforme: a review of natural history and management options. *Neurosurg Focus* 20(4): E3, 2006

14) Hsieh PC, Chandler JP, Bhangoo S, Panagiotopoulos K, Kalapurakal JA, Marymont MH, Cozzens JW, Levy RM, Salehi S: Adjuvant gamma knife stereotactic radiosurgery at the time of tumor progression potentially improves survival for patients with glioblastoma multiforme. *Neurosurgery* 57: 684–692, 2005

15) Ikuta S, Muragaki Y, Maruyama T, Ogata H, Iseki H: [Assessment of effect and toxicity of temozolomide combined with radiation therapy for newly-diagnosed glioblastoma in Japan]. *Tokyo Joshi Ika Daigaku Zasshi* 79: 510–515, 2009 (Japanese)

16) Iseki H, Nakamura R, Muragaki Y, Suzuki T, Chernov M, Hori T, Takakura K: Advanced computer-aided intraoperative technologies for information-guided surgical management of gliomas: Tokyo Women's Medical University experience. *Minim Invasive Neurosurg* 51: 285–291, 2008

17) Iuchi T, Hatano K, Narita Y, Kodama T, Yamaki T, Osato K: Hypofractionated high-dose irradiation for the treatment of malignant astrocytomas using simultaneous integrated boost technique by IMRT. *Int J*

Radiat Oncol Biol Phys 64: 1317–1324, 2006

18) Kondziolka D, Flickinger JC, Bissonette DJ, Bozik M, Lunsford LD: Survival benefit of stereotactic radiosurgery for patients with malignant glial neoplasms. *Neurosurgery* 41: 776–785, 1997

19) Lacroix M, Abi-Said D, Fourney DR, Gokaslan ZL, Shi W, DeMonte F, Lang FF, McCutcheon IE, Hassenbusch SJ, Holland E, Hess K, Michael C, Miller D, Sawaya R: A multivariate analysis of 416 patients with glioblastoma multiforme: prognosis, extent of resection, and survival. *J Neurosurg* 95: 190–198, 2001

20) Laperriere N, Zuraw L, Cairncross G: Radiotherapy for newly diagnosed malignant glioma in adults: A systematic review. *Radiother Oncol* 64: 259–273, 2002

21) Louis DN, Ohgaki H, Wiestler OD, Cavenee WK (eds): *WHO Classification of Tumours of the Central Nervous System.* Lyon, IARC, 2007

22) Lutz K, Radbruch A, Wiestler B, Baumer P, Wick W, Bendszus M: Neuroradiological response criteria for high-grade gliomas. *Clin Neuroradiol* 21: 199–205, 2011

23) McDonald MW, Shu HKG, Curran WJ Jr, Crocker IR: Pattern of failure after limited margin radiotherapy and temozolomide for glioblastoma. *Int J Radiat Oncol Biol Phys* 79: 130–136, 2011

24) Mikuni N, Miyamoto S: Surgical treatment of glioma: extent of resection applying functional neurosurgery. *Neurol Med Chir (Tokyo)* 50: 720–726, 2010

25) Milano MT, Okunieff P, Donatello RS, Mohile NA, Sul J, Walter KA, Korones DN: Patterns and timing of recurrence after temozolomide-based chemoradiation for glioblastoma. *Int J Radiat Oncol Biol Phys* 78: 1147–1155, 2010

26) Monjazeb AM, Ayala D, Jensen C, Case LD, Bourland JD, Ellis TL, McMullen KP, Chan MD, Tatter SB, Lesser GJ, Shaw EG: A Phase I dose escalation study of hypofractionated IMRT field-in-field boost for newly diagnosed glioblastoma multiforme. *Int J Radiat Oncol Biol Phys* 82: 743–748, 2012

27) Muragaki Y, Iseki H, Maruyama T, Kawamata T, Yamane F, Nakamura R, Kubo O, Takakura K, Hori T: Usefulness of intraoperative magnetic resonance imaging for glioma surgery. *Acta Neurochir Suppl* 98: 67–75, 2006

28) Muragaki Y, Iseki H, Maruyama T, Tanaka M, Shinohara C, Suzuki T, Yoshimitsu K, Ikuta S, Hayashi M, Chernov M, Hori T, Okada Y, Takakura K: Information-guided surgical management of gliomas using low-field-strength intraoperative MRI. *Acta Neurochir Suppl* 109: 67–72, 2011

29) Muragaki Y, Maruyama T, Iseki H, Tanaka M, Shinohara C, Takakura K, Tsuboi K, Yamamoto T, Matsumura A, Matsutani M, Karasawa K, Shimada K, Yamaguchi N, Nakazato Y, Sato K, Uemae Y, Ohno T, Okada Y, Hori T: Phase I/IIa trial of autologous formalin-fixed tumor vaccine concomitant with fractionated radiotherapy for newly diagnosed glioblastoma. *J Neurosurg* 115: 248–255, 2011

30) Muragaki Y, Maruyama T, Nakamura R, Iseki H, Kubo O, Takakura K, Hori T: [Information-guided surgery for glioma removal]. *No Shinkei Geka Journal* 15: 384–395, 2006 (Japanese)

31) Murakami R, Hirai T, Nakamura H, Furusawa M, Nakaguchi Y, Uetani H, Kitajima M, Yamashita Y: Recurrence patterns of glioblastoma treated with postoperative radiation therapy: relationship between extent of resection and progression-free interval. *Jpn J Radiol* 30: 193–197, 2012

32) Nagashima T, Matsutani M, Nakamura O, Tanaka Y: [Regrowth pattern of glioblastoma multiforme after radiotherapy]. *Gan No Rinsho* 35: 1272–1276, 1989 (Japanese)

33) Nakagawa K, Aoki Y, Fujimaki T, Tago M, Terahara A, Karasawa K, Sakata K, Sasaki Y, Matsutani M, Akanuma A: High-dose conformal radiotherapy influenced the pattern of failure but did not improve survival in glioblastoma multiforme. *Int J Radiat Oncol Biol Phys* 40: 1141–1149, 1998

34) Oh J, Sahgal A, Sanghera P, Tsao MN, Davey P, Lam K, Symons S, Aviv R, Perry JR: Glioblastoma: patterns of recurrence and efficacy of salvage treatments. *Can J Neurol Sci* 38: 621–625, 2011

35) Oppitz U, Maessen D, Zunterer H, Richter S, Flentje M: 3D-recurrence-patterns of glioblastomas after CT-planned postoperative irradiation. *Radiother Oncol* 53: 53–57, 1999

36) Pan H, Alksne J, Mundt AJ, Murphy KT, Cornell M, Kesari S, Lawson JD: Patterns of imaging failures in glioblastoma patients treated with chemoradiation: a retrospective study. *Med Oncol* Epub 2011 Nov 23

37) Paravati AJ, Heron DE, Landsittel D, Flickinger JC, Mintz A, Chen YF, Huq MS: Radiotherapy and temozolomide for newly diagnosed glioblastoma and anaplastic astrocytoma: Validation of Radiation Therapy Oncology Group—recursive partitioning analysis in the IMRT and temozolomide era. *J Neurooncol* 104: 339–349, 2011

38) Proescholdt MA, Macher C, Woertgen C, Brawanski A: Level of evidence in the literature concerning brain tumor resection. *Clin Neurol Neurosurg* 107: 95–98, 2005

39) Sanai N, Polley MY, McDermott MW, Parsa AT, Berger MS: An extent of resection threshold for newly diagnosed glioblastomas. *J Neurosurg* 115: 3–8, 2011

40) Shibui S: Randomized controlled trial on malignant brain tumors—activities of the Japan Clinical Oncology Group-Brain Tumor Study Group. *Neurol Med Chir (Tokyo)* 44: 220–221, 2004

41) Shuto T, Matsunaga N, Suinaga J, Yoshizumi T, Tuzuki S, Ootake M: [Role of gamma knife treatment for glioblastoma]. *Nippon Kagaku Ryoho Gakkai Zasshi* 37: 1024–1026, 2010 (Japanese)

42) Smith MM, Thompson JE, Castillo M, Cush S, Mukherji SK, Miller CH, Quattrocchi KB: MR of recurrent high-grade astrocytomas after intralesional immunotherapy. *AJNR Am J Neuroradiol* 17: 1065–1071,

1996

43) Sneed PK, Gutin PH, Larson DA, Malec MK, Phillips TL, Prados MD, Scharfen CO, Weaver KA, Wara WM: Patterns of recurrence of glioblastoma multiforme after external irradiation followed by implant boost. *Int J Radiat Oncol Biol Phys* 29: 719–727, 1994

44) Stewart LA: Chemotherapy in adult high-grade glioma: A systematic review and meta-analysis of individual patient data from 12 randomised trials. *Lancet* 359: 1011–1018, 2002

45) Stummer W, Reulen HJ, Meinel T, Pichlmeier U, Schumacher W, Tonn JC, Rohde V, Oppel F, Turowski B, Woiciechowsky C, Franz K, Pietsch T: Extent of resection and survival in glioblastoma multiforme: identification of and adjustment for bias. *Neurosurgery* 62: 564–576, 2008

46) Stupp R, Hegi ME, Mason WP, van den Bent MJ, Taphoorn MJ, Janzer RC, Ludwin SK, Allgeier A, Fisher B, Belanger K, Hau P, Brandes AA, Gijtenbeek J, Marosi C, Vecht CJ, Mokhtari K, Wesseling P, Villa S, Eisenhauer E, Gorlia T, Weller M, Lacombe D, Cairncross JG, Mirimanoff RO: Effects of radiotherapy with concomitant and adjuvant temozolomide versus radiotherapy alone on survival in glioblastoma in a randomised phase III study: 5-year analysis of the EORTC-NCIC trial. *Lancet Oncol* 10: 459–466, 2009

47) Stupp R, Mason WP, van den Bent MJ, Weller M, Fisher B, Taphoorn MJ, Belanger K, Brandes AA, Marosi C, Bogdahn U, Curschmann J, Janzer RC, Ludwin SK, Gorlia T, Allgeier A, Lacombe D, Cairncross JG, Eisenhauer E, Mirimanoff RO: Radiotherapy plus concomitant and adjuvant temozolomide for glioblastoma. *N Engl J Med* 352: 987–996, 2005

48) Takakura K, Abe H, Tanaka R, Kitamura K, Miwa T, Takeuchi K, Yamamoto S, Kageyama N, Handa H, Mogami H, Nishimoto A, Uozumi T, Matsutani M, Nomura K: Effects of ACNU and radiotherapy on malignant glioma. *J Neurosurg* 64: 53–57, 1986

49) Tanaka M, Ino Y, Nakagawa K, Tago M, Todo T: High-dose conformal radiotherapy for supratentorial malignant glioma: A historical comparison. *Lancet Oncol* 6: 953–960, 2005

50) Tsien C, Moughan J, Michalski JM, Gilbert MR, Purdy J, Simpson J, Kressel JJ, Curran WJ, Diaz A, Mehta MP: Phase I three-dimensional conformal radiation dose escalation study in newly diagnosed glioblastoma: Radiation Therapy Oncology Group trial 98–03. *Int J Radiat Oncol Biol Phys* 73: 699–708, 2009

51) van den Bent MJ, Carpentier AF, Brandes AA, Sanson M, Taphoorn MJ, Bernsen HJ, Frenay M, Tijssen CC, Grisold W, Sipos L, Haaxma-Reiche H, Kros JM, van Kouwenhoven MC, Vecht CJ, Allqeier A, Lacombe D, Gorlia T: Adjuvant procarbazine, lomustine, and vincristine improves progression-free survival but not overall survival in newly diagnosed anaplastic oligodendrogliomas and oligoastrocytomas: a randomized European Organization for Research and Treatment of Cancer phase III trial. *J Clin Oncol* 24: 2715–2722, 2006

52) Vogelbaum MA, Jost S, Aghi MK, Heimberger AB, Sampson JH, Wen PY, Macdonald DR, Van den Bent M, Chang SM: Application of novel response/progression measures for surgically delivered therapies for gliomas: Response Assessment in Neuro-Oncology (RANO) Working Group. *Neurosurgery* 70: 234–244, 2012

53) Westphal M, Hilt DC, Bortey E, Delavault P, Olivares R, Warnke PC, Whittle IR, Jaaskelainen J, Ram Z: A Phase 3 trial of local chemotherapy with biodegradable carmustine (BCNU) wafers (Gliadel wafers) in patients with primary malignant glioma. *Neuro Oncol* 5: 79–88, 2003

54) Wick W, Stupp R, Beule AC, Bromberg J, Wick A, Ernemann U, Platten M, Marosi C, Mason WP, van den Bent M, Weller M, Rorden C, Karnath HO: A novel tool to analyze MRI recurrence patterns in glioblastoma. *Neuro Oncol* 10: 1019–1024, 2008

Address reprint requests to: Yoshihiro Muragaki, MD, PhD, Faculty of Advanced Techno-Surgery, Institute of Advanced Biomedical Engineering and Science, Tokyo Women's Medical University, 8-1 Kawada-cho, Shinjuku-ku, Tokyo 162-8666, Japan.
e-mail: ymuragaki@abmes.twmu.ac.jp

Immunohistochemical analysis-based proteomic subclassification of newly diagnosed glioblastomas

Kazuya Motomura,[1] Atsushi Natsume,[1,11] Reiko Watanabe,[2] Ichiro Ito,[2] Yukinari Kato,[3] Hiroyuki Momota,[1] Ryo Nishikawa,[4] Kazuhiko Mishima,[4] Yoko Nakasu,[5] Tatsuya Abe,[6] Hiroki Namba,[7] Yoichi Nakazato,[8] Hiroshi Tashiro,[2] Ichiro Takeuchi,[9] Tsutomu Mori[10] and Toshihiko Wakabayashi[1]

[1]Department of Neurosurgery, Nagoya University School of Medicine, Nagoya; [2]Division of Diagnostic Pathology, Shizuoka Cancer Center, Shizuoka; [3]Molecular Tumor Marker Research Team, Faculty of Medicine, The Oncology Research Center, Advanced Molecular Epidemiology Research Institute, Yamagata University, Yamagata; [4]Department of Neurosurgery, Saitama Medical University International Center, Saitama; [5]Department of Neurosurgery, Shizuoka Cancer Center, Shizuoka; [6]Department of Neurosurgery, Oita University School of Medicine, Oita; [7]Department of Neurosurgery, Hamamatsu University School of Medicine, Hamamatsu; [8]Department of Human Pathology, Gunma University School of Medicine, Gunma; [9]Department of Engineering, Nagoya Institute of Technology, Nagoya; [10]Department of Human Lifesciences, Fukushima Medical University School of Nursing, Fukushima, Japan

Recent gene expression and copy number profilings of glioblastoma multiforme (GBM) by The Cancer Genome Atlas (TCGA) Research Network suggest the existence of distinct subtypes of this tumor. However, these approaches might not be easily applicable in routine clinical practice. In the current study, we aimed to establish a proteomics-based subclassification of GBM by integrating their genomic and epigenomic profiles. We subclassified 79 newly diagnosed GBM based on expression patterns determined by comprehensive immunohistochemical observation in combination with their DNA copy number and DNA methylation patterns. The clinical relevance of our classification was independently validated in TCGA datasets. Consensus clustering identified the four distinct GBM subtypes: Oligodendrocyte Precursor (OPC) type, Differentiated Oligodendrocyte (DOC) type, Astrocytic Mesenchymal (AsMes) type and Mixed type. The OPC type was characterized by highly positive scores of Olig2, PDGFRA, p16, p53 and synaptophysin. In contrast, the AsMes type was strongly associated with strong expressions of nestin, CD44 and podoplanin, with a high glial fibrillary acidic protein score. The median overall survival of OPC-type patients was significantly longer than that of the AsMes-type patients (19.9 vs 12.8 months). This finding was in agreement with the Oncomine analysis of TCGA datasets, which revealed that PDGFRA and Olig2 were favorable prognostic factors and podoplanin and CD44 were associated with a poor clinical outcome. This is the first study to establish a subclassification of GBM on the basis of immunohistochemical analysis. Our study will shed light on personalized therapies that might be feasible in daily neuropathological practice. (*Cancer Sci* 2012; 103: 1871–1879)

G lioblastoma multiforme (GBM) is one of the most common and highly malignant brain tumors in the primary central nervous system in adults. GBM was one of the first tumor types registered in The Cancer Genome Atlas (TCGA), which is a project that catalogs genomic abnormalities involved in the development of cancer.[1,2] The techniques currently used in TCGA study for the detection of abnormalities include gene expression profiling, copy number variation profiling, single-nucleotide polymorphism genotyping, genome-wide methylation profiling,[3] microRNA profiling[4] and exon sequencing. Since the publication of the first TCGA Network paper,[1] several groups within the TCGA network have presented the results of highly detailed analyses of GBM. Verhaak et al.[5] recently subclassified GBM into Proneural, Neural, Classical and Mesenchymal subtypes by integrating multidimensional data on gene expression, somatic mutations and DNA copy number. The main features of the Proneural class are focal amplification of *PDGFRA*, *IDH1* mutation, and *TP53* mutation and/or loss of heterozygosity. Moreover, high expression of genes associated with oligodendrocyte development, such as *PDGFRA*, *NKX2-2* and *OLIG2*, were also associated with this subtype. The Neural subtype is characterized by the expression of neuron markers, such as *NEFL*, *GABRA1*, *SYT1* and *SLC12A5*. The Classical subtype features high *EGFR* expression associated with chromosome 7 amplification and low expression of *p16INK4A* and *p14ARF*, resulting from a focal 9p21.3 homozygous deletion. Neural stem cell markers, such as nestin, as well as components of the Notch and Sonic hedgehog signaling pathways, are highly expressed in the Classical type. The Mesenchymal subtype is characterized by focal hemizygous deletions at 17q11.2 that contains *NF1* and high expression of *YKL-40* (*CHI3L1*), *MET*, *CD44* and *MERTK*. This classification of GBM using gene expression profiles (TCGA) may address the important issue of the inability to define different patient outcomes on the basis of histopathological features. For ultimately establishing a simple classification of groups of patients with GBM according to clinicopathological factors, a protein-based immunohistochemical approach, which is routinely used in most neuropathology laboratories, needs to be applied to avoid more complex molecular biology techniques.[6]

In the present study, we analyzed 79 archival GBM samples by immunohistochemistry using antibodies against 16 proteins selected based on Verhaak's classification for immunohistochemical analysis-based GBM subclassification, including Proneural (Olig2, IDH1-R132H,[7] p53, PDGFRA and PDGFB), Neural (synaptophysin), Classical (p16, EGFR, Hes-1 and nestin) and Mesenchymal types (VEGF, YKL-40, CD44 and podoplanin [PDPN]), as well as high glial fibrillary acidic protein (GFAP) and Ki-67, and incorporated the results into the existing genomic and epigenomic data for these samples. We successfully identified clinically relevant subtypes that partially overlap the Verhaak subgroups.

Materials and Methods

Tumor samples. Samples from 79 consecutive patients with newly diagnosed GBM from several academic tertiary-care neurosurgical institutions were collected. All the samples were collected from GBM patients treated with temozolomide

[11]To whom correspondence should be addressed.
E-mail: anatsume@med.nagoya-u.ac.jp

(TMZ). Paraffin-embedded surgical samples were collected for immunohistochemical analysis. All of the specimens had been fixed in 10% formalin. Three neuropathologists (Y.N., R.W. and I.I.) independently confirmed the GBM diagnosis according to WHO guidelines.[8,9]

Matched fresh-frozen tissue samples were also obtained. DNA was prepared as described previously.[10] All the patients provided their written informed consent for molecular studies of their tumor at each participating hospital. The study had the approval of each of the ethics committees of the Nagoya University Hospital, Shizuoka Cancer Center, Saitama Medical University Hospital, Oita University Hospital and Hamamatsu Medical University Hospital (title, "Genetic analysis associated with brain tumor"). This study complied with all the provisions of the Declaration of Helsinki.

Immunohistochemical analysis. Immunohistochemical analysis was performed as previously described.[11] The antibodies used in the present study are summarized in Table S1. For each immunostained slide, the percentage of positively stained GBM cells on a given slide was evaluated and scored, as shown in Table S2. This procedure was performed by two pathologists (R.W. and I.I.), and scores were decided through a consensus. This process was performed twice, and the final scores were determined at the second round before clustering analysis.

Multiplex ligation-dependent probe amplification. Multiplex ligation-dependent probe amplification (MLPA) was used for determining allelic losses and gains of the gene in the tumor samples. The analysis was performed using the SALSA MLPA kit P088-B1 and P105-C1 in accordance with the manufacturer's protocol (MRC Holland, Amsterdam, the Netherlands).[12–15] All the procedures were performed as described previously.[10]

Pyrosequencing. Tumor DNA was modified with bisulfate by using the EpiTect bisulfite kit (Qiagen, Courtaboeuf Cedex, France). Pyrosequencing technology was used to determine the methylation status of the CpG island region of MGMT, as described previously.[10,16,17]

TP53 and IDH1/IDH2 sequencing. Direct sequencing of *TP53* exons 5–8, which contain mutation hot spots in gliomas, and *IDH1/2* was performed as previously described.[10,18–20] For IDH sequencing, 129 and 150-bp fragments spanning the sequences encoding the catalytic domains of *IDH1* (including codon 132) and *IDH2* (including codon 172), respectively, were amplified.

Oncomine data analysis. An independent set of 401 GBM mRNA expression profiles was analyzed by using the Oncomine Premium Research Edition to assess subtype reproducibility. Details of the standardized normalization techniques and statistical calculations can be found on the Oncomine website (https://www.oncomine.com).

Statistical analysis. To identify distinct GBM subclasses, we applied consensus clustering to our immunohistochemical data.[21] Consensus clustering has been used in many recent biomedical studies because it can estimate the statistical stability of the identified clusters.[5] Within the consensus clustering, *K*-means clustering with the Euclidean distance metric was used as the basic clustering option. For *K* ranging from 2 to 5, the *K*-means clustering was run over 10 000 iterations with a subsampling ratio of 0.8 for estimating the consensus matrix. For the purpose of visualization and cluster identification, hierarchical clustering with the Euclidean distance metric and the complete linkage option was applied to the estimated consensus matrix. The identified clusters were validated and confirmed using consensus cluster dependence factor plot analysis[21] and silhouette analysis.[22] To visualize the four identified clusters, principal component analysis (PCA) was applied to the immunohistochemical data and 3-D ellipsoids representing the covariance structure of each cluster were drawn in the 3-D plots of the first three principal components. Most of the statistical analyses (except the 3-D plot, which was generated by JMP ver.9.0) were performed using R.[23] We used a Kruskal–Wallis rank test to analyze the differences between the four GBM subgroups, and the pairwise differences in the expressions of 16 proteins and genetic/epigenetic alterations between each subgroup and the other three subgroups. The differences between the GBM subtypes with $P < 0.005$ were considered to be statistically significant in a more stringent manner, as the four clusters themselves are determined by the expression of these proteins and genetic/epigenetic alterations. Statistical analysis of survival was performed using the statistical software SPSS version 17.0 for Windows (SPSS, Chicago, IL, USA). Survival was estimated using the Kaplan–Meier method and survival curves were compared using the log-rank test.

Results

Patient characteristics. The summary of the GBM patient and treatment characteristics is shown in Table S3. All 79 patients received surgical treatment followed by standard TMZ-based chemotherapy and conventional radiation therapy, with daily concurrent TMZ at 75 mg/m^2 throughout the course of the radiation therapy.[24]

This study population included 50 male and 29 female patients aged 13–84 years (median age, 61 years). The median preoperative Eastern Cooperative Oncology Group performance status (ECOG PS) score at diagnosis was one (range, 0 –4); the preoperative ECOG PS score was <1 in the case of 48 patients (60.8%). All the tumors were located in the supratentorial region: 60 tumors (75.9%) were located in the superficial area (cortical or subcortical area), and 19 (24.1%) were located in deep anatomical structures such as the basal ganglia and corpus callosum. Surgical gross total resection (GTR) was achieved in 24 patients (30.4%), and non-GTR was performed in 55 patients (69.6%).

Consensus clustering subclassifies four subtypes. The GBM subtypes identified by consensus clustering are shown in Figure 1, with clustering stability increasing from $K = 2$ to $K = 4$, but not to $K = 5$ (Figs 1,2). Furthermore, the identified clusters were confirmed on the basis of their positive silhouette width,[22] indicating higher similarity to their own class than to a member of any other class (Fig. 3).

According to the results, the 79 GBM cases examined were basically classified into four clusters: clusters I (nine cases), II (17 cases), III (14 cases) and IV (39 cases), depending on the branch length, which represents the correlation between the scoring data and the similarity in GBM tumor samples (Fig. 4). This analysis identified four discrete groups of sample sets that differed markedly in GBM protein expression. The 3-D ellipsoid of each cluster in PCA in Figure 5 also suggests the clear separations of each cluster. All the scores for the immunohistochemical analysis and genetic/epigenetic data lists for all the analyses are available in Table S4.
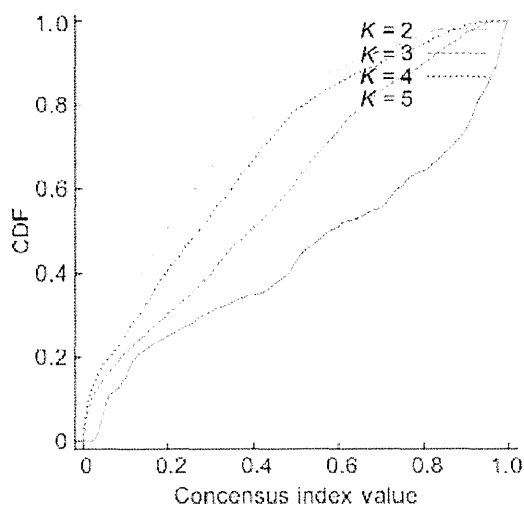
These protein groups were named according to the distribution and biological function of the representative protein expressions of Olig2, IDH1-R132H, PDGFRA, p16, EGFR, Hes-1, nestin, CD44, PDPN and GFAP; that is, Oligodendrocyte Precursor (OPC) type, Differentiated Oligodendrocyte (DOC) type, Astrocytic Mesenchymal (AsMes) type, and Mixed type. Figure 6 shows the immunohistochemical staining pattern in the 79 GBM cases, aligned according to the four identified clusters, indicating similarity in immunohistochemical staining patterns within each cluster.

Differentiated Oligodendrocyte type. All the samples clustered in this type showed high positivity for the oligodendroglial marker Olig2 and small round cell morphology (Table 1,
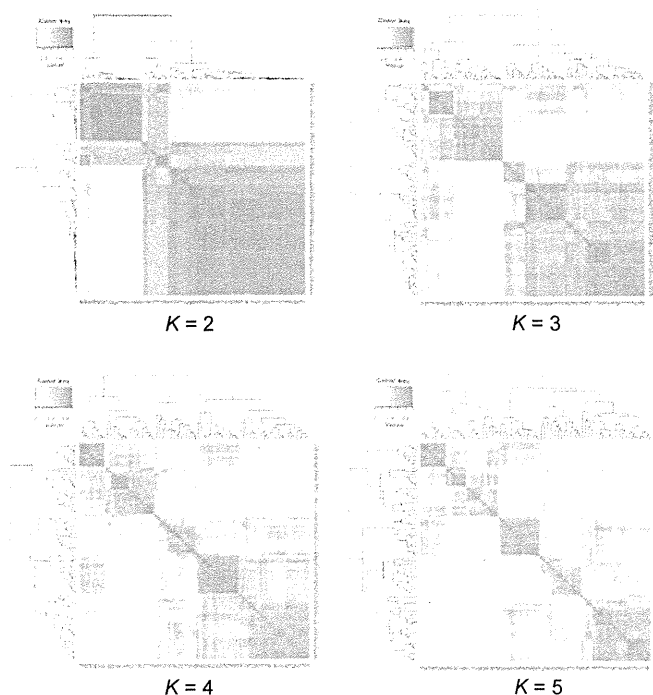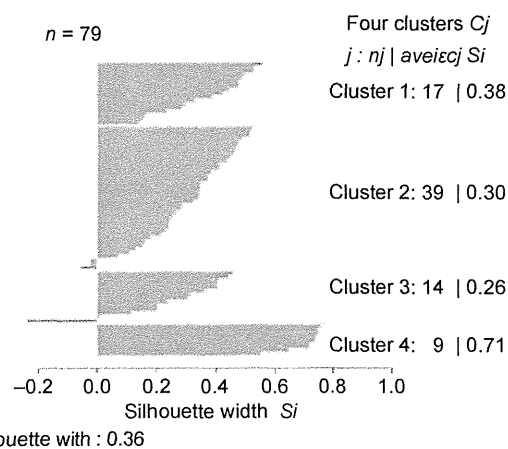
Fig. 1. Consensus matrix heat maps demonstrating the presence of several clusters within the 79 samples of GBM for $K = 2$ to $K = 5$ cluster assignments for each cluster method. The red areas identify the similarity between the samples and display samples clustered together across the bootstrap analysis.
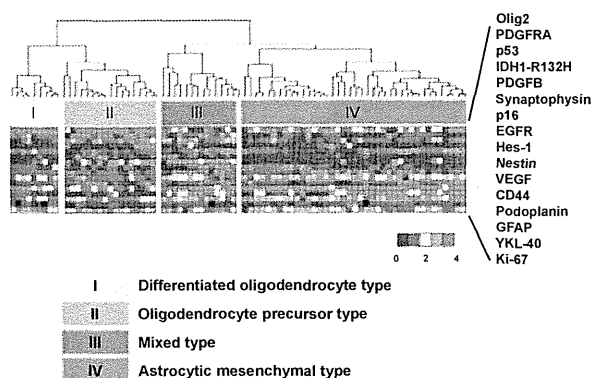

Fig. 2. Consensus clustering cluster dependence factor (CDF) for $K = 2$ to $K = 5$.

Fig. 3. Silhouette plot for identification of core samples.

I   Differentiated oligodendrocyte type

II   Oligodendrocyte precursor type

III Mixed type

IV   Astrocytic mesenchymal type

Fig. 4. Immunohistochemical analysis-based subgroups and comparison with genetic and epigenetic alterations. The heat map and dendrogram show the expression profiles of 16 proteins well characterized in glioblastoma multiforme (GBM) and demonstrate the significant pattern of differential expression among the four subgroups. The statistical significance of the differential protein expression was determined using one-way ANOVA.

Fig. 6). Furthermore, negativity for p53 and p16 was noted. GFAP was almost always negative in the tumor cell cytoplasm (Fig. 6). Genetically, 1p/19q co-deletion and *CDKN2A* loss were more frequently observed in this cluster than in the other clusters (Fig. 7). The presence of 1p/19q co-deletion was assessed if the DNA copy numbers at a minimum of three adjacent loci were less than 0.65 at 1p and 19q.

Oligodendrocyte Precursor type. This cluster was characterized by highly positive scores for PDGFRA, p16, and p53 in addition to a highly positive score for an oligodendroglial marker, Olig2 (Fig. 6). From the perspective that oligodendrocytes arise during development from oligodendrocyte precursors,

which can be identified by the expression of a number of antigens, including PDGFRA, this subgroup was named the Oligodendrocyte Precursor (OPC) type. On the contrary, few samples had high scores for nestin, CD44, and PDPN in this group (Table 1; Fig. 6). It is interesting that the genetic alterations were observed in *IDH1* mutations (23.5%) and *TP53* mutations (52.9%). These findings were consistent with the results of protein expression. Methylation of the MGMT promoter (41.2%) was most frequently detected in this cluster (Fig. 7).

Astrocytic Mesenchymal type. This type was generally characterized by: strong membranous and/or stromal positivity for CD44 and/or PDPN; cytoplasmic positivity for GFAP and/or nestin in tumor cells; total negativity for p16, except in the case of four patients; and sparse positivity for p53 (Table 1, Fig. 6). Morphologically, the tumor cells observed in the H&E-stained sections showed pleomorphism. In striking contrast to the OPC type, this type was also strongly associated with low levels of Olig2, IDH1-R132H, p53, p16 and PDGFRA, and rather strong GFAP expression (Table 1). These findings suggest that this cluster was strongly characterized by astrocytic features.

Genetically, *IDH1* and *TP53* mutations were rare in this group. Furthermore, methylation of the MGMT promoter (20.5%) was detected at a low frequency (Fig. 7).

Motomura *et al.*
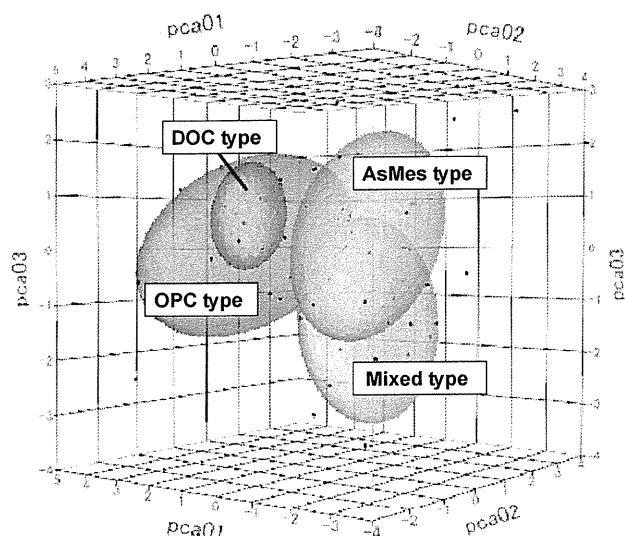
Fig. 5. Principal component analysis (PCA) of four glioblastoma multiforme (GBM) subtypes. Ellipsoid bodies represent two SD of the data distribution for each subgroup.

Mixed type. Compared with TCGA's Classical-type markers, frequent expressions of p16 (79%), EGFR (36%) and Hes-1 (64%), as well as a Proneural-type marker, p53 (64%), were predominant in this class (Table 1, Fig. 6).

Strong expression of the downstream Notch transcriptional target Hes-1 suggested that the prominent Notch-Hes-1 pathway was activated in this class. Furthermore, this cluster was characterized by positivity for CD44 and GFAP, and morphologically, by tumor cells with eosinophilic cytoplasm. This morphological characteristic was compatible with limited or scant positivity for Olig2. CD44 and PDPN were detected in many tumor cells.

In addition, this cluster had a genetically high frequency of *EGFR* amplification (57.1%) and low frequency of *CDKN2A* loss, and these findings are consistent with the protein expression data (Fig. 7). Thus, we named this cluster Mixed type because it shares characteristics of the OPC type and AsMes type or those of TCGA's Proneural and Classical types.

Morphological characteristics of the four types. On the H&E-stained sections, the morphological findings of the four types were fairly characteristic, although not specific (Fig. 8). In the DOC type, the tumor cells had small round or oval nuclei, scant cytoplasm and few cytoplasmic processes. The tumor cell nuclei showed a fine and diffuse chromatin (Fig. 8a,b). In some cases in which the tumor cells had faint processes, the cells tended to gather around vessels.

In the OPC type, in addition to small round or oval nucleated cells similar to those of the DOC type, there were scattered intermediate to large pleomorphic and/or multinucleated neoplastic cells, cells with vesicular chromatin, and/or cells with short spindle-shaped or irregularly-shaped nuclei that were slightly larger than the small round or oval cells (Fig. 8c,d).

In the AsMes type, many neoplastic cells had spindle-shaped nuclei and almost bipolar, distinct cytoplasmic processes. They were generally arranged in bundle-like and interlacing patterns. Some neoplastic cells had nuclei with vesicular open chromatin. The boundaries of the cytoplasmic processes were generally well defined (Fig. 8e,f).

In the Mixed type, there were scattered large pleomorphic cells on a background of intermediate or small cells. The latter background cells had irregularly-shaped nuclei and spindle-shaped cytoplasmic processes that were haphazardly arranged, in comparison with the bundle formations in the AsMes type (Fig. 8g,h).

Overview of the immunohistochemical data and genomic/epigenomic profiles across the four glioblastoma multiforme subtypes. We sought to select the most significant factors to distinguish the four GBM subgroups by a Kruskal–Wallis rank test. As indicated in Tables S5 and S6, the differences between the GBM subtypes showing $P < 0.005$ were considered to be statistically significant in a more stringent manner, as the four clusters themselves are determined by the expression of these proteins and genetic/epigenetic alterations. Of these, Olig2, p53, PDGFRA, synaptophysin, p16 and the *IDH1* mutation were positively correlated with the OPC type, whereas positive correlations with nestin, PDPN, CD44 and GFAP were predominant in the AsMes type. The DOC type showed a significant positive correlation with Olig2, and there was a significant positive correlation with the p16 expression in the Mixed type.

Proteomic clusters correlate with survival. The Kaplan–Meier survival analysis revealed that the four proteomic clusters differed significantly in their correlation with survival (Fig. 9 and Table 2). There were no significant differences in any of the clinical parameters (i.e. age, sex, preoperative ECOG PS, tumor location and extent of resection; Table S3) between the four cluster groups, as determined using the Fisher exact test.

It is interesting that the median overall survival (OS) associated with the OPC type was significantly longer (19.9 months [95% CI, 8.3–31.4]) than that of the patients with the AsMes type (12.8 months [95% CI, 10.0–15.7; $P = 0.041$]; Fig. 9). The difference was statistically significant, as determined by the log-rank test and univariate analysis. These findings are consistent with the OPC type being characterized by higher positive scores for IDH1-R132H (29%) in the immunohistochemical analysis and a high frequency of *IDH1* mutation (23.5%) in the genetic analysis, which are known to predict long-term survival.[25] Although the survival period of the patients in the Mixed type appeared to be the longest (median OS: 21.3 months [95% CI, 7.9–34.8]) among those of the other subgroups, the difference between these three subgroups was not statistically significant, presumably owing to the limited sample size in this study; the Kaplan–Meier curve of the DOC type (median OS: 14.8 months [95% CI, 2.6–27.0]) was similar to those of the OPC and Mixed types (Fig. 9).

Subgroup-specific outcome based on mRNA expression in The Cancer Genome Atlas datasets. An independent set of 401 GBM mRNA expression profiles was compiled from the Oncomine Premium Research Edition to assess subtype reproducibility. Among our selected 16 protein markers, information about the mRNA expressions of 12 markers and clinical outcomes could be obtained from TCGA brain dataset. IDH1-R132H, p53, p16 and Ki-67 were not available in the 401 GBM mRNA expression profiles of TCGA dataset because IDH1-R132H and p53 antibodies were used to detect mutation status, and this did not correlate with the mRNA expression of each gene. Moreover, because p16 protein expression correlates with the homozygous deletion of *CDKN2A*, we also excluded this protein from the analysis. In this analysis, the Olig2, PDGFB and PDGFRA mRNA expression levels were significantly low in the tumors of patients who died at 1 year compared with those who survived for 1 year after the treatment. Notably, PDGFRA was the most favorable prognostic factor among these factors ($P = 0.002$; Fig. 10 and Tables 3 and 4).

Furthermore, PDPN, CD44, YKL-40 and EGFR mRNA were significantly overexpressed in the tumors of the patients who died 1 year after the treatment. These results indicate that PDPN is significantly associated with a poor clinical outcome ($P = 0.0003$; Fig. 10).
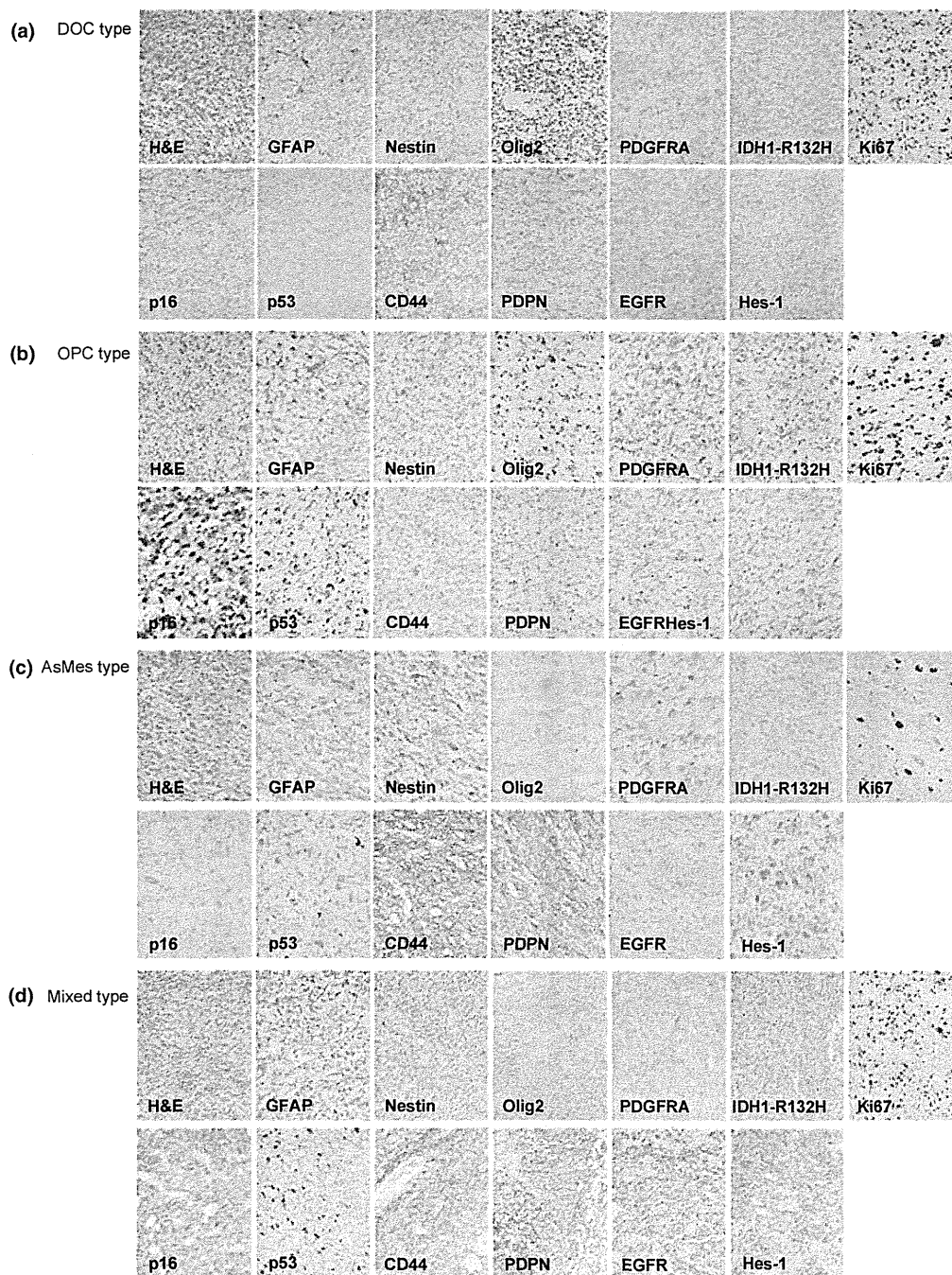
Fig. 6. Representative immunohistochemical images used in this study. (a) Differentiated Oligodendrocyte type (DOC type), glioblastoma multiforme (GBM) case.44. (b) Oligodendrocyte Precursor type (OPC type), GBM case.01. (c) Astorocytic Mesenchymal type (AsMes type), GBM case 03. (d) Mixed type, GBM case 04.

Discussion

A large number of studies have shown that GBM can be classified by gene and protein expression profiling.[5,26–28] The TCGA Research Network classifies GBM according to gene expression profiles into Proneural, Neural, Classical and Mesenchymal subtypes.[5] However, these transcriptomic approaches might not be easily applied in routine clinical practice because complicated techniques are necessary to perform several of the experiments. Compared with these approaches, an immunohistochemistry-based approach could have widespread utility in the clinical set-ting and lead to significantly improved patient stratification. The goal of the current study was to subclassify GBM using an immunohistochemical approach that is feasible in daily neuro-pathological practice, using a dataset from the TCGA Research Network as a reference. Our classification based on immunohistochemical analyses may enable the prediction of clinical chemo-sensitivity and survival in TMZ-treated patients with GBM.

Identification of four novel clusters by immunohistochemical analysis. We identified four novel clusters (OPC type, DOC type, AsMes type and Mixed type) with a considerably different expression profile of GBM tumors; to our knowledge, such an

Table 1. Frequency of positive score ≥3

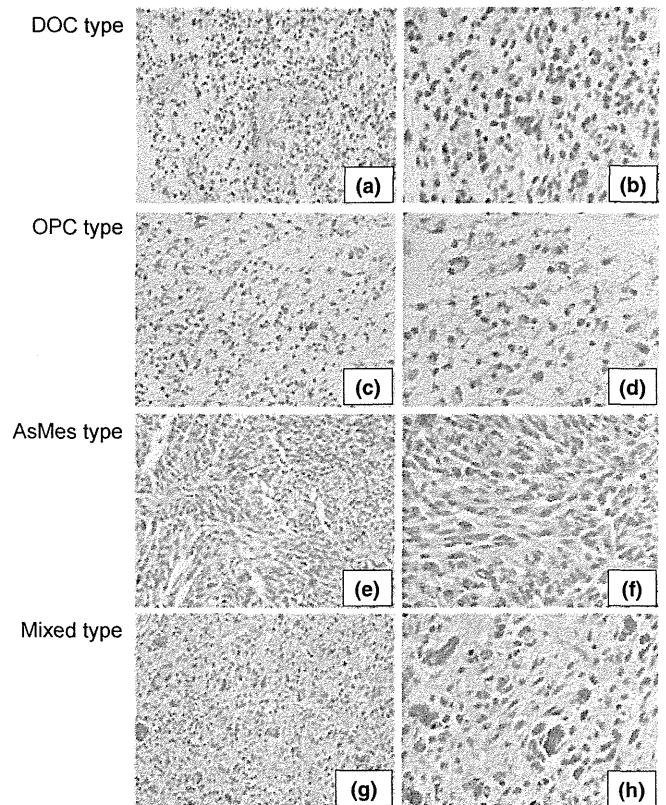| Proteins	DOC type (n = 9) (%)	OPC type (n = 17) (%)	Mixed type (n = 14) (%)	AsMes type (n = 39) (%)	Total
Proneural					
Olig2	9 (100)	14 (82)	4 (29)	16 (41)	43
IDH1-R132H	0 (0)	5 (29)	0 (0)	1 (3)	6
p53	1 (11)	9 (53)	9 (64)	5 (13)	24
PDGFRA	3 (33)	10 (59)	5 (36)	3 (8)	21
PDGFB	2 (22)	1 (6)	5 (35)	9 (23)	17
Neural					
Synaptophysin	0 (0)	3 (18)	3 (21)	0 (0)	6
Classical					
p16	0 (0)	9 (53)	11 (79)	2 (5)	22
EGFR	0 (0)	0 (0)	5 (36)	5 (13)	10
Hes-1	0 (0)	3 (17	9 (64)	11 (28)	23
Nestin	2 (22)	2 (12)	4 (29)	24 (62)	32
Mesenchymal					
VEGF	1 (11)	6 (35)	4 (29)	11 (28)	22
YKL-40	0 (0)	1 (6)	0 (0)	2 (5)	3
Podoplanin	0 (0)	0 (0)	4 (29)	18 (46	22
CD44	5 (56)	1 (6)	11 (79)	37 (95)	54
GFAP	0 (0	3 (18)	10 (71)	32 (82)	45
Ki-67	5 (56)	11 (65)	5 (29)	18 (46)	39

AsMes, astrocytic mesenchymal; DOC, differentiated oligodendrocyte; OPC, oligodendrocyte precursor.
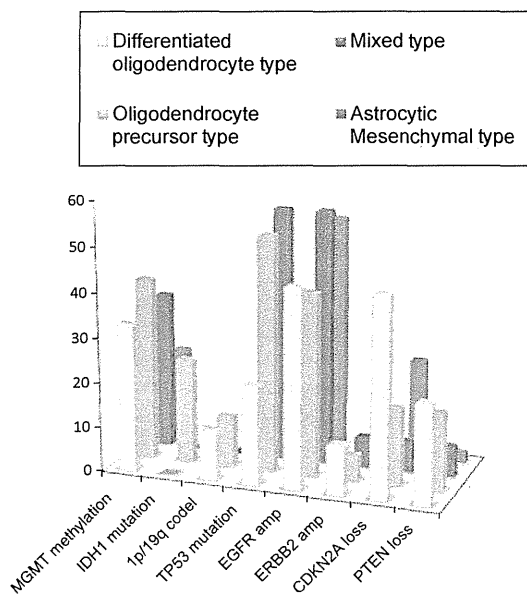

Fig. 7. Frequency and pattern of genetic and epigenetic alterations in four glioblastoma multiforme (GBM) subtypes.

Fig. 8. Morphological findings of four types on the H&E sections. In the Differentiated Oligodendrocyte (DOC) type (original magnification: (a) ×20; (b) ×40), the tumor cells have small round/oval nuclei and indistinct processes. In the Oligodendrocyte Precursor (OPC) type (original magnification: (c) ×20; (d) ×40), there are scattered intermediate to large pleomorphic and/or multinucleated cells. In the Astrocytic Mesenchymal (AsMes) type (original magnification: (e) ×20; (f) ×40), spindle-shaped cytoplasmic processes are distinct and form bundles in an interlacing fashion. In the Mixed type (original magnification: (g) ×20; (h) ×40), in the background of small-sized to intermediate-sized spindle-shaped cells arranged in a haphazard fashion, there are several pleomorphic large cells.
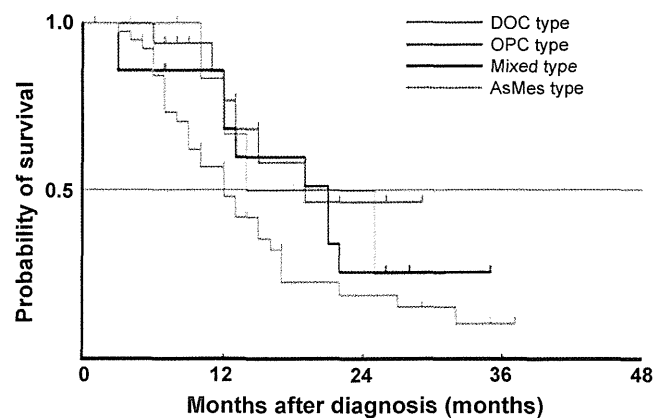

Fig. 9. Kaplan–Meier estimates of overall survival (OS) for all the glioblastoma multiforme (GBM) patients (n = 79) separated into four subgroups.

expression profile has not been described elsewhere. However, the limitation of unsupervised clustering, which does not guarantee a clinically relevant classification, must be considered. Among the four clusters, the OPC and AsMes types in particular showed unique immunohistochemical patterns.

In addition, the survival patterns of the patients with GBM tumors classified into these types were significantly different. The OPC type was characterized by a favorable outcome and high positivity for Olig2, PDGFRA and IDH1-R132H on the immunohistochemical staining. The Kaplan–Meier log-rank test revealed that the OPC type was associated with a median

OS of 19.9 months (Fig. 9). This is possibly a result of the high positive score for IDH1-R132H, which is well recognized as a predictive biomarker and may influence this favorable sur-

Table 2. Median overall survival of each of the four glioblastoma multiforme subtypes

	Median overall survival (months)	95% CI
Proteomic clusters		
OPC type	19.9†	8.3–31.4
DOC type	14.8	2.6–27.0
Mixed type	21.3	7.9–34.8
AsMes type	12.8	10.0–15.7

†The median overall survival of the OPC type was significantly longer (19.9 months [95% CI, 8.3–31.4]) than that of the AsMes type (12.8 months [95% CI, 10.0–15.7]) (P = 0.041). AsMes, astrocytic mesenchymal; DOC, differentiated oligodendrocyte. OPC, oligodendrocyte precursor.

A. No value (45)
B. Alive at 1 year (162)
C. Dead at 1 year (194)
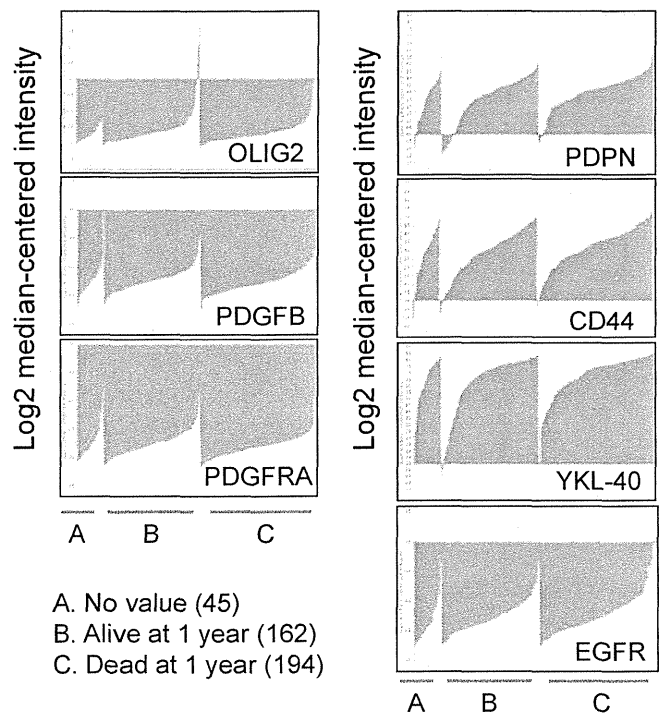
Fig. 10. Seven factors among our 16 markers that are correlated significantly with clinical outcomes from TCGA datasets. B and C show the log2 median-centered intensity of tumors of patients who were alive or dead at 1 year, respectively.

vival in GBM. Oligodendrocyte precursor cells are thought to develop from neural stem cells through multiple genetic and morphological changes.[29] Oligodendrocyte precursor cells express Olig1, Olig2, Sox10, Nkx2.2[30] and PDGFRA.[31,32] In particular, PDGFRA signaling is known to regulate the proliferation of oligodendrocyte precursor cells during neonatal development and regeneration in adulthood.[33]

In contrast, the characteristics of the AsMes type were high positivity for PDPN and CD44 in the stroma and GFAP in tumor cells. PDPN is a mucin-like transmembrane sialoglycoprotein putatively involved in migration, invasion, metastasis and malignant progression of several tumors, such as squamous cell carcinomas, mesothelioma and testicular tumors.[34–36] Furthermore, PDPN expression is thought to be associated with malignant progression of astrocytomas.[37] A study showed the presence of putative binding sites for NF1 within the basic transcription factor of the PDPN promoter lesion,[38] suggesting that NF1 negatively downregulates the expression of PDPN. CD44 is a major cell surface hyaluronan receptor and cancer stem cell marker that has been implicated in the progression of various cancer types.[39] Recently, CD44 was found to be upregulated in a broad range of GBM, and its elevated expression was correlated with poor prognosis.[40] An interesting finding is that CD44 and PDPN colocalize on cell surface protrusions in carcinoma cells, and the PDPN-CD44 interaction is important for driving directional cell migration in malignant tumors.[41]

The DOC type was clustered adjacent to the OPC type, suggesting that these clusters are closer to each other than to the other two clusters. A unique characteristic of the DOC type was that high positivity for Olig2 was observed in all the tumor sections in this cluster, whereas the positivity for the other markers was unremarkable. Genetically, the highest frequency of 1p/19q co-deletion, which refers to the combination of both 1p and 19q partial loss, and both hemizygous and homozygous deletions of the *CDKN2A* gene were observed in this class. This type is a heterogeneous group consisting of either 1p/19q co-deletion or *CDKN2A*-loss tumors. Taken together, this class may be differentiated into an oligodendroglioma-like lineage from oligodendrocyte precursor cells. The Mixed type was indeed mixed between the OPC and AsMes types. Moreover, PCA revealed that this type was a combination of the OPC and AsMes types.

Comparison with The Cancer Genome Atlas subclassification and validation of The Cancer Genome Atlas brain dataset. Mutations of the *IDH1* and *TP53* genes and high expression levels and high copy numbers of *PDFGRA* were frequently observed in the Proneural subtype advocated by Phillips and Verhaak,[5,26] suggesting that the OPC type is similar to the Proneural type. Striking characteristics common to the OPC type and the DOC type were high Olig2 expression and low

Table 3. Underexpression: dead at 1 year

Gene symbol	Reporter ID	t-test	P-value	Q-value	Fold change
OLIG2	213824_at	−2.105792	0.018113879	0.220443238	−1.0732534
PDGFB	217112_at	−2.3643584	0.009313148	0.188830637	−1.0354494
PDGFRA	211533_at	−2.8829412	0.002104464	0.141673037	−1.0440509

Table 4. Overexpression: dead at 1 year

Gene symbol	Reporter ID	t-test	P-value	Q-value	Fold change
PDPN	204879_at	3.4651806	3.04E-04	0.322990973	1.4722846
CD44	204490_s_at	2.6668687	0.004021729	0.527154075	1.296043
YKL-40	209395_at	2.2250252	0.013421925	0.672091602	1.3869164
EGFR	211551_at	1.8736842	0.030904011	0.840823061	1.0449007

313

expression levels of GFAP. However, the OPC type was characterized by higher positive scores for PDGFRA, p16, p53 and synaptophysin. The OPC type may be a mixture of Proneural and Neural subtypes.

In the Classical subtype, *EGFR* amplification and *CDKN2A* homozygous deletions were the frequent genetic alterations observed. Moreover, components of the nestin and Notch signaling pathways were highly expressed. According to our classification, overexpression of EGFR and the downstream effector of Notch signaling Hes-1 were most frequently observed in the Mixed type. Deletion of *CDKN2A* and downregulation of p16 were characteristic of the DOC type, and strong nestin expression was most frequently observed in the AsMes type. The Mesenchymal subtype was characterized by high expression levels of YKL-40 and MET and high frequency of *NF1* mutation/deletion. In our dataset, the mesenchymal markers PDPN and CD44 were highly expressed in the AsMes type, which is also characterized by strong GFAP expression. The combination of higher activity of mesenchymal and astrocytic markers is suggestive of an epithelial-to-mesenchymal transition.

In the present study, the outcomes of the patients with the OPC and AsMes types were significantly different. Contrary to Verhaak's classification, the outcomes of the patients with the OPC and AsMes types, on the basis of our classification, were significantly different.

Furthermore, we could easily distinguish these two subtypes using PDGFRA, p16, p53, PDPN and CD44, as well as the routinely used proteins, GFAP, Olig2, synaptophysin and nestin. The ability to discriminate these two subtypes will contribute to the development of different therapeutic approaches for each GBM subtype.

Although there were no independent validation samples of paraffin-embedded sections of GBM, determining the associa-

tion between the expressions of these markers and the outcomes in 406 TCGA brain datasets would be of interest. Of note, Oncomine suggested that the overexpressions of PDPN and CD44 were associated with poor prognosis, and high expression levels of Olig2 and PDGFRA in tumor cells significantly improved the patient outcome. We are currently conducting a prospective randomized clinical trial, the Japan Clinical Oncology Group Study 0911, to validate the additive efficacy of interferon-β in 120 patients with newly diagnosed GBM.[42,43] It is anticipated that his clinical trial will validate our immunohistochemical approach.

In conclusion, the data obtained by expression profiling of 79 GBM tumors based on immunohistochemical studies suggest the existence of four proteomic subgroups of GBM tumors. To the best of our knowledge, this is the first study to establish the subclassification of GBM on the basis of immunohistochemical analysis. Among the four subtypes, the patients with the OPC type showed favorable outcomes. To develop more effective and less toxic GBM treatment regimens, it is necessary to identify and correctly classify the proteomic subtypes, as well as understand the underlying oncogenic driving pathways for each type.

Acknowledgments

Disclosure Statement

References

1 Network CGAR. Comprehensive genomic characterization defines human glioblastoma genes and core pathways. *Nature* 2008; **455**: 1061–8.
2 Parsons DW, Jones S, Zhang X *et al.* An integrated genomic analysis of human glioblastoma multiforme. *Science* 2008; **321**: 1807–12.
3 Noushmehr H, Weisenberger DJ, Diefes K *et al.* Identification of a CpG island methylator phenotype that defines a distinct subgroup of glioma. *Cancer Cell* 2010; **17**: 510–22.
4 Kim TM, Huang W, Park R, Park PJ, Johnson MD. A developmental taxonomy of glioblastoma defined and maintained by MicroRNAs. *Cancer Res* 2011; **71**: 3387–99.
5 Verhaak RG, Hoadley KA, Purdom E *et al.* Integrated genomic analysis identifies clinically relevant subtypes of glioblastoma characterized by abnormalities in PDGFRA, IDH1, EGFR, and NF1. *Cancer Cell* 2010; **17**: 98–110.
6 Northcott PA, Korshunov A, Witt H *et al.* Medulloblastoma comprises four distinct molecular variants. *J Clin Oncol* 2011; **29**: 1408–14.
7 Kato Y, Jin G, Kuan CT, McLendon RE, Yan H, Bigner DD. A monoclonal antibody IMab-1 specifically recognizes IDH1R132H, the most common glioma-derived mutation. *Biochem Biophys Res Commun* 2009; **390**: 547–51.
8 Louis DN, Ohgaki H, Wiestler OD *et al.* The 2007 WHO classification of tumours of the central nervous system. *Acta Neuropathol* 2007; **114**: 97–109.
9 Kleihues P, Cavenee WK. *WHO Classification of Tumours of the Central Nervous System.* Lyon: WHO Press, 2000.
10 Motomura K, Natsume A, Kishida Y *et al.* Benefits of interferon-beta and temozolomide combination therapy for newly diagnosed primary glioblastoma with the unmethylated MGMT promoter: a multicenter study. *Cancer* 2011; **117**: 1721–30.
11 Watanabe R, Nakasu Y, Tashiro H *et al.* O6-methylguanine DNA methyltransferase expression in tumor cells predicts outcome of radiotherapy plus concomitant and adjuvant temozolomide therapy in patients with primary glioblastoma. *Brain Tumor Pathol* 2011; **28**: 127–35.
12 Franco-Hernandez C, Martinez-Glez V, Alonso ME *et al.* Gene dosage and mutational analyses of EGFR in oligodendrogliomas. *Int J Oncol* 2007; **30**: 209–15.

13 Jeuken J, Cornelissen S, Boots-Sprenger S, Gijsen S, Wesseling P. Multiplex ligation-dependent probe amplification: a diagnostic tool for simultaneous identification of different genetic markers in glial tumors. *J Mol Diagn* 2006; **8**: 433–43.
14 Schouten JP, McElgunn CJ, Waaijer R, Zwijnenburg D, Diepvens F, Pals G. Relative quantification of 40 nucleic acid sequences by multiplex ligation-dependent probe amplification. *Nucleic Acids Res* 2002; **30**: e57.
15 Martinez-Glez V, Franco-Hernandez C, Lomas J *et al.* Multiplex ligation-dependent probe amplification (MLPA) screening in meningioma. *Cancer Genet Cytogenet* 2007; **173**: 170–2.
16 Natsume A, Wakabayashi T, Tsujimura K *et al.* The DNA demethylating agent 5-aza-2'-deoxycytidine activates NY-ESO-1 antigenicity in orthotopic human glioma. *Int J Cancer* 2008; **122**: 2542–53.
17 Oi S, Natsume A, Ito M *et al.* Synergistic induction of NY-ESO-1 antigen expression by a novel histone deacetylase inhibitor, valproic acid, with 5-aza-2'-deoxycytidine in glioma cells. *J Neurooncol* 2009; **92**: 15–22.
18 Nobusawa S, Watanabe T, Kleihues P, Ohgaki H. IDH1 mutations as molecular signature and predictive factor of secondary glioblastomas. *Clin Cancer Res* 2009; **15**: 6002–7.
19 Fults D, Brockmeyer D, Tullous MW, Pedone CA, Cawthon RM. p53 mutation loss of heterozygosity on chromosomes 17 and 10 during human astrocytoma progression. *Cancer Res* 1992; **52**: 674–9.
20 Hartmann C, Meyer J, Balss J *et al.* Type and frequency of IDH1 and IDH2 mutations are related to astrocytic and oligodendroglial differentiation and age: a study of 1,010 diffuse gliomas. *Acta Neuropathol* 2009; **118**: 469–74.
21 Monti S, Tamayo P, Mesirov J, Golub T. Consensus clustering: a resampling-based method for class discovery and visualization of gene expression microarray data. *Machine Learning* 2003; **52**: 91–118.
22 Rousseeuw PJ. Silhouettes – A graphical aid to the interpretation and validation of cluster-analysis. *J Comput Appl Math* 1987; **20**: 53–65.
23 Team RDC. *A Language and Environment for Statistical Computing.* Vienna, Austria: R Foundation for Statistical Computing, 2008.
24 Stupp R, Mason WP, van den Bent MJ *et al.* Radiotherapy plus concomitant and adjuvant temozolomide for glioblastoma. *N Engl J Med* 2005; **352**: 987–96.
25 Yan H, Parsons DW, Jin G *et al.* IDH1 and IDH2 mutations in gliomas. *N Engl J Med* 2009; **360**: 765–73.

26 Phillips HS, Kharbanda S, Chen R *et al.* Molecular subclasses of high-grade glioma predict prognosis, delineate a pattern of disease progression, and resemble stages in neurogenesis. *Cancer Cell* 2006; **9**: 157–73.

27 Brennan C, Momota H, Hambardzumyan D *et al.* Glioblastoma subclasses can be defined by activity among signal transduction pathways and associated genomic alterations. *PLoS One* 2009; **4**: e7752.

28 Gravendeel LA, Kouwenhoven MC, Gevaert O *et al.* Intrinsic gene expression profiles of gliomas are a better predictor of survival than histology. *Cancer Res* 2009; **69**: 9065–72.

29 Nicolay DJ, Doucette JR, Nazarali AJ. Transcriptional control of oligodendrogenesis. *Glia* 2007; **55**: 1287–99.

30 Hu BY, Du ZW, Li XJ, Ayala M, Zhang SC. Human oligodendrocytes from embryonic stem cells: conserved SHH signaling networks and divergent FGF effects. *Development* 2009; **136**: 1443–52.

31 Levine JM, Reynolds R, Fawcett JW. The oligodendrocyte precursor cell in health and disease. *Trends Neurosci* 2001; **24**: 39–47.

32 Nishiyama A, Lin XH, Giese N, Heldin CH, Stallcup WB. Co-localization of NG2 proteoglycan and PDGF alpha-receptor on O2A progenitor cells in the developing rat brain. *J Neurosci Res* 1996; **43**: 299–314.

33 Rao RC, Boyd J, Padmanabhan R, Chenoweth JG, McKay RD. Efficient serum-free derivation of oligodendrocyte precursors from neural stem cell-enriched cultures. *Stem Cells* 2009; **27**: 116–25.

34 Kato Y, Kaneko M, Sata M, Fujita N, Tsuruo T, Osawa M. Enhanced expression of Aggrus (T1alpha/podoplanin), a platelet-aggregation-inducing factor in lung squamous cell carcinoma. *Tumour Biol* 2005; **26**: 195–200.

35 Kato Y, Sasagawa I, Kaneko M, Osawa M, Fujita N, Tsuruo T. Aggrus: a diagnostic marker that distinguishes seminoma from embryonal carcinoma in testicular germ cell tumors. *Oncogene* 2004; **23**: 8552–6.

36 Kato Y, Kaneko MK, Kuno A *et al.* Inhibition of tumor cell-induced platelet aggregation using a novel anti-podoplanin antibody reacting with its platelet-aggregation-stimulating domain. *Biochem Biophys Res Commun* 2006; **349**: 1301–7.

37 Mishima K, Kato Y, Kaneko MK, Nishikawa R, Hirose T, Matsutani M. Increased expression of podoplanin in malignant astrocytic tumors as a novel molecular marker of malignant progression. *Acta Neuropathol* 2006; **111**: 483–8.

38 Hantusch B, Kalt R, Krieger S, Puri C, Kerjaschki D. Sp1/Sp3 and DNA-methylation contribute to basal transcriptional activation of human podoplanin in MG63 versus Saos-2 osteoblastic cells. *BMC Mol Biol* 2007; **8**: 20.

39 Stamenkovic I, Yu Q. Shedding light on proteolytic cleavage of CD44: the responsible sheddase and functional significance of shedding. *J Invest Dermatol* 2009; **129**: 1321–4.

40 Xu Y, Stamenkovic I, Yu Q. CD44 attenuates activation of the hippo signaling pathway and is a prime therapeutic target for glioblastoma. *Cancer Res* 2010; **70**: 2455–64.

41 Martin-Villar E, Fernandez-Munoz B, Parsons M *et al.* Podoplanin associates with CD44 to promote directional cell migration. *Mol Biol Cell* 2010; **21**: 4387–99.

42 Wakabayashi T, Kayama T, Nishikawa R *et al.* A multicenter phase I trial of interferon-beta and temozolomide combination therapy for high-grade gliomas (INTEGRA Study). *Jpn J Clin Oncol* 2008; **38**: 715–8.

43 Wakabayashi T, Kayama T, Nishikawa R *et al.* A multicenter phase I trial of combination therapy with interferon-beta and temozolomide for high-grade gliomas (INTEGRA study): the final report. *J Neurooncol* 2011; **104**: 573–7.

Supporting Information

Additional Supporting Information may be found in the online version of this article:

Table S1. Antibodies and immunostaining conditions.

Table S2. Scoring system for immunohistochemical positivity used in this study.

Table S3. Clinical characteristics of the four GBM subtypes.

Table S4. Scores of all immunohistochemical analysis and genetic/epigenetic data lists for all the analyses.

Table S5. Significant pairwise correlation coefficients derived from the Kruskal–Wallis rank test of the expressions of 16 proteins in the four GBM subgroups.

Table S6. Significant pairwise correlation coefficients derived from the Kruskal–Wallis rank test of the genetic and epigenetic alterations in the four GBM subgroups.

Please note: Wiley-Blackwell are not responsible for the content or functionality of any supporting materials supplied by the authors. Any queries (other than missing material) should be directed to the corresponding author for the article.

Original Article

Benefits of Interferon-β and Temozolomide Combination Therapy for Newly Diagnosed Primary Glioblastoma With the Unmethylated MGMT Promoter

A Multicenter Study

Kazuya Motomura, MD[1]; Atsushi Natsume, MD[1,2]; Yugo Kishida, MD[1]; Hiroyuki Higashi[3]; Yutaka Kondo, MD[4];
Yoko Nakasu, MD[5]; Tatsuya Abe, MD[6]; Hiroki Namba, MD[7]; Kenji Wakai, MD[8]; and Toshihiko Wakabayashi, MD[1]

BACKGROUND: The aim of the current study was to catalog genomic and epigenomic abnormalities in newly diagnosed glioblastoma patients and determine the correlation among clinical, genetic, and epigenetic profiles and clinical outcome. **METHODS:** This study retrospectively included 68 consecutive patients who underwent surgical treatment and received standard radiotherapy with temozolomide (TMZ)-based chemotherapy. Of a total of 68 patients, 39 patients (57.4%) received interferon (IFN)-β in combination of TMZ. **RESULTS:** The genetic and epigenetic alterations frequently observed were EGFR amplification (51.5%), TP53 mutation (33.8%), CDKN2A loss (32.4%), TP53 loss (16.2%), methylation of the MGMT promoter (33.8%) and IDH1 mutation (5.9%). Multivariate analysis revealed that methylated MGMT promoter and the combination of TMZ and IFN-β were independent prognostic factors associated with survival. The median survival time (MST) of the patients who received the combination of IFN-β and TMZ was significantly greater with 19.9 months as compared to the TMZ alone group (12.7 months). Notably, in even patients whose tumors had unmethylated MGMT promoter, the MST prolonged to 17.2 months when receiving TMZ with IFN-β, compared to 12.5 months in those receiving TMZ without IFN-β. **CONCLUSIONS:** Taken together, addition of IFN-β for newly diagnosed primary GBM achieved a favorable outcome, particularly in patients with unmethylated MGMT promoter. *Cancer* 2011;117:1721-30. © 2010 American Cancer Society.

KEYWORDS: IDH1, MGMT methylation, glioblastoma, interferon-β, temozolomide.

Glioblastoma multiforme (GBM) is one of the most frequent primary brain tumors in the central nervous system in adults and is highly malignant, with a median survival time of about one year from diagnosis. This is despite aggressive treatment, surgery, postoperative radiotherapy, and adjuvant chemotherapy. An international randomized trial by the European Organization for Research and Treatment of Cancer/National Cancer Institute of Canada (EORTC/NCIC) comparing radiotherapy alone and concomitant radiotherapy and temozolomide (TMZ) clearly attested the benefits of adjuvant TMZ chemotherapy for GBM patients.[1] Since then, TMZ has been the current first-line chemotherapeutic agent for GBM.

A subanalysis in this trial showed the effectiveness of epigenetic silencing of the MGMT gene by promoter methylation with longer survival in patients with primary GBM; it also suggested the benefits of combining chemotherapy using TMZ with radiotherapy.[2]

Furthermore, there have been recent attempts to comprehensively profile GBM genes by The Cancer Genome Atlas (TCGA) project and other groups.[3,4] Some genetic aberrations in GBM, such as *TP53* mutation or deletion, *NF1* deletion or mutation, and *ERBB2* mutation, have been found to be more common than previously reported. In addition, novel molecular markers, such as frequent mutations of the *IDH1* and *IDH2* genes in secondary GBM have been discovered.[5-7] These findings on mutations, genomic and epigenomic aberrations, and transcriptomal features in GBM might aid in understanding the classification of GBM and its further potential clinical implications.

However, the TCGA project included GBM patients who received surgical treatment, and detailed information on adjuvant chemoradiotherapy was not provided. Therefore, the close relationship between the gene profile provided by TCGA and chemotherapy regimens remains unknown.[3]

In this current study, we aimed to determine the correlation between clinical, genetic, and epigenetic profiles, and clinical outcome in newly diagnosed GBM patients who received TMZ-based chemotherapy. Interestingly, we found a significant beneficial outcome in patients receiving TMZ in addition to IFN-β. Moreover, our study discovered that GBM patients with the unmethylated O^6-methylguanine-DNA methyltransferase (MGMT) promoter, in particular, showed benefits from IFN-β.

MATERIALS AND METHODS
Patient population
We retrospectively reviewed 68 consecutive patients with newly diagnosed primary GBM who underwent surgical treatment at several academic tertiary-care neurosurgical institutions: Nagoya University Hospital, Hamamatsu University Hospital, Oita University Hospital, and Shizuoka Cancer Center from May 2006 through June 2010 after TMZ was approved as the treatment agent for malignant gliomas by the National Ministry of Health and Welfare of Japan. The diagnosis of GBM was established by histological confirmation according to the WHO guidelines[8,9] independently by at least two expert neuropathologists. The clinical, operative, and hospital course records were reviewed. Information collected from clinical notes included patient demographics, pre- and postoperative neuroimaging, and adjuvant therapy. Preoperative Eastern Cooperative Oncology Group performance status

(ECOG PS) scores were assigned by the clinician at the time of evaluation and were available in the chart for review for all patients. The study was approved by the institutional review board at each participating hospital and complied with all provisions of the Declaration of Helsinki.

Treatment
Radiotherapy
After undergoing surgery, the patients received focal external-beam radiotherapy by conventional radiation planning to approximately 60 Gray (Gy) ($\pm$5% total dose), with daily concurrent TMZ at 75 mg/m^2 throughout the course of radiotherapy.

Chemotherapy
All patients received the standard Stupp regimen.[1] In the absence of grade 3 or 4 hematological excessive toxicity, TMZ administration was continued until clinical or radiological evidence of disease progression was observed. Of these 68 patients, 39 patients (57.4%) received adjuvant IFN-β treatment (Table 1). Patients in Nagoya University and Oita University received chemotherapy consisting of IFN-β. There were no significant differences in any of the clinical parameters and genetic, epigenetic parameters (i.e., age, sex, preoperative PS, tumor location, extent of resection, genetic and epigenetic alterations between the institutions using regimen with and without IFN-β. The IFN-β chemotherapy regimen comprised 3 million international units (MIU)/body administered intravenously on alternate days during radiotherapy and TMZ-induction chemotherapy.[10,11] At the end of the induction period, after a 4-week interval, the patients were administered 3 MIU/body of IFN-β on the first morning every 4 weeks during TMZ maintenance chemotherapy. In the case of tumor progression, salvage or second-line therapy was administered at the investigators' discretion; most patients received additional chemotherapy.

Response Evaluation During Treatment
Both radiological and clinical findings were used to evaluate the response. Follow-up magnetic resonance imaging (MRI) was performed for alternate cycles. If the MRI showed continued increase in enhancement, the case was considered as tumor progression. If re-resection was performed for a recurrent mass lesion, histological interpretation formed the basis for definitive diagnosis (treatment-related necrosis vs recurrent tumor).

317

Table 1. Clinical Characteristics[a]{TC}

Parameter	No. of Patients	%
	n=68	
Age(y)		
Median	55.0	
Range	12-84	
<40	12	17.6
≥40, <60	24	35.3
≥60	32	47.1
Sex		
Male	41	60.3
Female	27	39.7
Preoperative ECOG performance status		
Median	1	
Range	0-3	
Preoperative ECOG performance status		
≤1	45	66.2
>1	23	33.8
Tumor location		
Superficial	50	73.5
Deep	18	26.5
Surgery		
GTR	24	35.3
Non-GTR	44	64.7
Chemotherapy		
TMZ only	29	42.6
TMZ+ IFN-β	39	57.4

ECOG indicates Eastern Cooperative Oncology Group; PS, performance status; GTR, macroscopic (gross) total removal; TMZ, temozolomide.

Tumor Samples and DNA Extraction

All patients provided their written informed consent for molecular studies of their tumor, and the protocol was approved by the ethics committee at each center. Sixty-eight brain tumor specimens were obtained at the time of first surgical resection.

Tumor tissue samples were immediately frozen and stored at −80°C until the extraction of genomic DNA. DNA was prepared using the QIAmp DNA Mini kit (Qiagen, Hilden, Germany) according to the manufacturer's instructions. Placental DNA was used as the normal control. The amount of DNA obtained from the tumor was sufficient for the subsequent genomic and epigenomic analyses.

Multiplex Ligation-Dependent Probe Amplification

Multiplex ligation-dependent probe amplification (MLPA) was used for the determination of allelic losses and gains of the gene in the tumor samples. The analysis was performed using the SALSA MLPA KIT P088-B1 and P105-C1 in accordance with the manufacturer's protocol (MRC Holland, Amsterdam, Netherland).[12-15] Information regarding the probe sequences and ligation sites can be found at www.mlpa.com. Amplification products were separated on an ABI® 3130 × 1 Genetic Analyzer (Applied Biosystems, Foster City, CA) and quantified with Genemapper 4.0 software (Applied Biosystems). Duplicate experiments were performed to obtain accurate MLPA values. Data analysis was performed with an original Excel-based program based on MRC-Holland's procedures. Normalization for sample data was first performed on control probes, and each tumor sample was then normalized using the data on 2 control samples, using peripheral blood DNA. Single regression for control and tumor data slope correction was performed. Abnormal/normal ratio limits were set at 0.65 and 1.3. Statistical analysis was performed using the same Coffalyser software.

Pyrosequencing

Tumor DNA was modified with bisulfate using the EpiTect bisulfite kit (Qiagen, Courtaboeuf Cedex, France). Pyrosequencing technology was used to determine the methylation status of the CpG island region of MGMT as described previously.[16,17] We used the touchdown PCR method. The primer sequences used were the MGMT forward primer, 5′-TTGGTAAATTAAGGTATAGAGTTTT-3′, and the MGMT biotinylated reverse primer, 5′-AAA CAATCTACGCATCCT-3′. PCR included a denaturation step at 95°C for 30 s, followed by annealing at various temperatures for 45 s, and extension at 72°C for 45 s. After PCR, the biotinylated PCR product was purified as recommended by the manufacturer. In brief, the PCR product was bound to Streptavidin Sepharose HP (Amersham Biosciences, Uppsala, Sweden), and the Sepharose beads containing the immobilized PCR product were purified, washed, and denatured using 0.2 N NaOH solution and washed again. Next, 0.3 mM pyrosequencing primer was annealed to the purified single-stranded PCR product, and pyrosequencing was performed using the PSQ HS 96 Pyrosequencing System (Pyrosequencing, Westborough, MA). The pyrosequencing primer was 5′-GGAAGTTGGGAAGG-3′. Methylation quantification was performed using the provided software.

TP53 and IDH1/IDH2 Sequencing

Direct sequencing of the *TP53* exons 5 to 8 and *IDH1/IDH2* was performed as previously described.[7,18,19] The primer sequences are listed in Table 2.

318

Table 2. List of Primer Sequences for Direct DNA Sequencing{TC}

Gene name	Exon		Sequence
TP53	Exon 5	F	5'-TTATCTGTTCACTTGTGCCC-3'
		R	5'-ACCCTGGGCAACCAGCCCTG-3'
	Exon 6	F	5'-ACGACAGGGCTGGTTGCCCA-3',
		R	5'-CTCCCAGAGACCCCAGTTGC-3'
	Exon 7	F	5'-GGCCTCATCTTGGGCCTGTG-3'
		R	5'-CAGTGTGCAGGGTGGCAAGT-3'
	Exon 8	F	5'-CTGCCTCTTGCTTCTCTTTT-3'
		R	5'-TCTCCTCCACCGCTTCTTGT-3'.
IDH1		F	5'-CGGTCTTCAGAGAAGCCATT-3'
		R	5'-GCAAAATCACATTATTGCCAAC-3'
IDH2		F	5'-AGCCCATCATCTGCAAAAAC-3'
		R	5'-CTAGGCGAGGAGCTCCAGT-3'.

F indicates forward primer; R, reverse primer;.

For IDH sequencing, a fragment 129 bp in length, spanning the sequence encoding the catalytic domain of *IDH1*, including codon 132, and a fragment 150 bp in length spanning the sequence encoding the catalytic domain of *IDH2*, including codon 172, were amplified. We applied touchdown PCR, using the standard buffer conditions: it comprised 5 ng of DNA and AmpliTaq Gold DNA Polymerase (Applied Biosystems) run for 16 cycles with denaturation at 95°C for 30 s, annealing at 65 to 57°C (decreasing by 0.5°C per cycle) for 30 s, and extension at 72°C for 60 s in a total volume of 12.5 μl and add 30 cycles with denaturation at 95°C for 30 s, annealing at 55°C for 30 s, and extension at 72°C for 60 s, ending with at 72°C for 7 min to complete extension.

Direct sequencing was performed using BigDye Terminator v1.1 Cycle Sequencing Kit (Applied Biosystems). The reactions were carried out using an ABI 3100 Genetic Analyzer (Applied Biosystems).

Statistical Analysis

Statistical analysis was performed using the statistical software SPSS for Windows, version 17.0 (SPSS Inc, Chicago, Ill). The Mann-Whitney U test, χ^2 test, and Fisher exact test were used to test for association of clinical variables and molecular markers. Survival was estimated by using the Kaplan-Meier method, and survival curves were compared by using the log-rank test. Progression-free survival (PFS) was calculated from the day of first surgery until tumor progression, death, or end of follow up. Overall survival (OS) was calculated from the day of first surgery until death or the end of follow up. Univariate and multivariate analyses were performed to test the potential influence of baseline characteristics on survival. The effect

of each single molecular marker on PFS and OS was investigated using the Cox proportional hazards model, adjusting for the major clinical prognostic factors, including age at diagnosis (<40 vs ≥40, <60 vs ≥60 years), ECOG performance status score (ECOG PS; ≤1 vs >1), extent of resection (macroscopic [gross] total resection [GTR] vs non-GTR), tumor location (superficial vs deep), MGMT promoter methylation status, chromosome 1p loss of heterozygosity (LOH), 19qLOH, *PTEN* loss, *CDKN2A* loss, *TP53* loss and mutation, *ERBB2* amplification, *EGFR* amplification, *IDH1* and *IDH2* mutation, and adjuvant therapy (with IFN-β vs without IFN-β). Factors with no significant association with survival, at a level of more than 0.05 in the multivariate analysis, were eliminated. The remaining factors in the multivariate proportional hazard model ($P <.05$) were considered to be independent predictors of survival.

To assess for the treatment effects of TMZ with IFN-β versus TMZ without IFN-β for overall survival (OS), the hazard ratio was computed using a proportional hazard model by baseline characteristics in stratified analysis.

RESULTS

Clinical Parameters

Between May 2006 and June 2010, 68 consecutive patients newly diagnosed with primary GBM were registered in this study. Their clinical characteristics are summarized in Table 1. This study group comprised 41 men and 27 women aged 12-84 years (median, 55). The median preoperative ECOG PS score at diagnosis was 1 (range, 0-3); the preoperative ECOG PS score was <1 in 45 patients (66.2%). All tumors were located in the supratentorial region: 50 tumors were located in the superficial area (cortical or subcortical area), and 18 were located in deep anatomical structures such as the basal ganglia and corpus callosum. No tumor was noted in the optic nerve, olfactory nerve, and pituitary gland on pretreatment MRI. No tumor dissemination was detected by MRI. Surgical GTR was achieved in 24 patients (35.3%), and 44 patients underwent non-GTR (64.7%). None of the patients had concurrent active malignancy, and the baseline organ function before chemotherapy was as follows: absolute WBC $\geq3000/mm^3$ or neutrophil count $\geq1,500/mm^3$, platelet count $\geq100,000/mm^3$, hemoglobin ≥8.0 g/dl, AST less than 2.5 × the upper limit of normal (ULN), total bilirubin 2 × ULN, and creatinine 2 × ULN, and electrocardiogram showing no serious
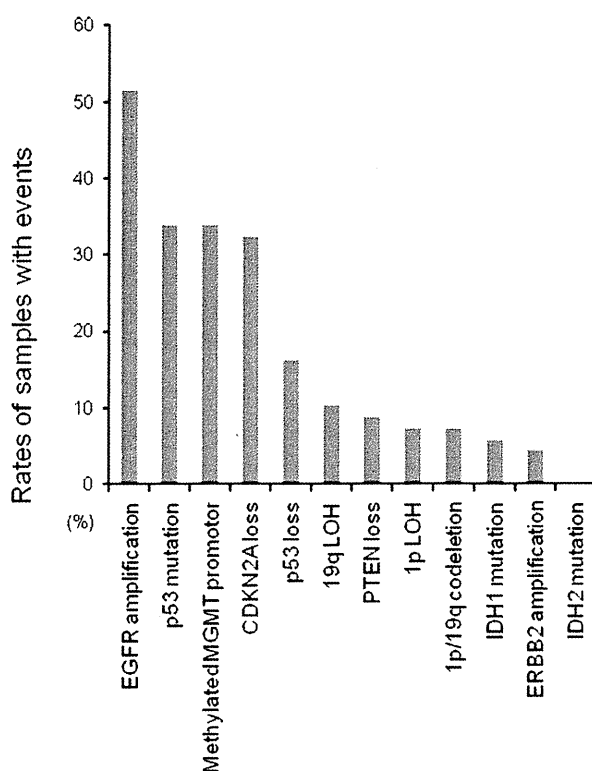
Figure 1. Frequency and pattern of genetic and epigenetic alterations in newly diagnosed primary glioblastoma multiforme (GBM).

arrhythmia and no serious ischemic heart disease. All patients received the standard Stupp regimen,[1] and among these, 39 patients were received combination treatment with IFN-β, as described in the method section.

Frequency of Genetic and Epigenetic Alterations

Of 68 cases, we could obtain sufficient genetic and epigenetic information in all cases. We used direct sequencing for TP53 and IDH1/2. We employed MLPA for the analysis of 1p/19q LOH, loss of TP53, PTEN and CDKN2A, and amplification of ERBB2 and EGFR. MLPA is a multiplex PCR method that detects abnormal copy numbers of up to 50 different genomic DNA sequences simultaneously. When comparing MLPA to FISH, MLPA not only has the advantage of being a multiplex technique but also one in which very small (50-70 nt) sequences are targeted, enabling MLPA to identify the frequent, single gene aberrations that are very small to be detected by FISH. Furthermore, for the detection of EGFR amplification, MLPA can examine exons 1-8, 13, 16, and 22, while pre-

viously reported real-time PCR covers only exons 2, 17, and 25. In our preliminary experiments, MLPA was found to be approximately 80% consistent with the real-time PCR method (data not shown). Notably, the methylation status of the MGMT promoter was analyzed by quantitative pyrosequencing technology. Although methylation-specific PCR analysis of MGMT promoter methylation is a widely applicable biomarker for the clinical setting, it is non quantitative and bears a risk of false-positive or false-negative results, especially when the DNA quality and/or quantity is low. Recent attempts to remedy some of these deficiencies have led to the development of an alternative sequence-based approach for methylation analysis, known as pyrosequencing. Pyrosequencing yields continuous methylation values ranging from 0-100%. Based on our comparisons with standard methylation-specific PCR and immunohistochemical study using the anti-MGMT antibody, we determined 14% as the threshold distinguishing unmethylation and methylation of the MGMT promoter in a given tumor.

As indicated in Figure 1 and Table 3, the alterations frequently observed were EGFR amplification (51.5%), TP53 mutation (33.8%), CDKN2A loss (32.4%), TP53 loss (16.2%), methylation of the MGMT promoter (33.8%), and IDH1 mutation (5.9%). These findings were consistent with those in previous reports.[3,9,20,21]

Clinical, Genetic, and Epigenetic Parameters Associated With Survival in GBM Patients

The median follow-up time was 16.7 months (range, 3.4-46.7 months). The median PFS for all patients was 9.2 months (95% confidence interval [CI], 5.7-12.7). The median OS of all patients was 17.1 months (95% CI, 15.5-18.7) (Figure 2A). The log-rank tests demonstrated that tumor localization ($P = .032$), the MGMT methylation status ($P = .029$), and TP53 mutation or loss ($P = .035$) were associated with the OS of patients with GBM (Figure 2B-D). These findings were similar to univariate analysis, where deep location ($P = .035$), unmethylated MGMT promoter ($P = .033$) and TP53 mutation or loss ($P = .038$) were identified as candidate variables for poorer OS (Figure 2). In contrast, well-established prognostic factors such as age, ECOG PS, and the extent of tumor resection did not influence the outcome in this clinical setting. Next, we established multivariate survival models for OS. The model was designed to consider each of these factors without considering the interaction terms. The independent prognostic factors for OS were methylated MGMT promoter ($P = .016$).

320